Evaluation of Microencapsulated Silicone Oils as Oxygen Carriers in the Production of Dihydroxyacetone by *Gluconobacter oxydans*

by Francesco Munaretto, B. Eng

Department of Chemical Engineering
McGill University, Montreal, Canada

A thesis submitted to the Faculty of Graduate Studies and Research in partial fulfilment of the requirements for the degree of Master of Engineering.

 April 1996

ISBN 0-612-19877-4

Canada

ABSTRACT

Two types of oxygen carrying particles were formed: a 200cs silicone oil, microencapsulated within a nylon membrane, and a solid silicone elastomer microsphere. These oxygen carriers had mean diameters of 0.1 and 1 mm respectively. Free cell cultures of *Gluconobacter oxydans* performing a bioconversion of glycerol to dihydroxyacetone in a non-growth medium were supplied with oxygen solely from the oxygen carriers. The production of DHA by the culture was used as a bioprobe to evaluate the oxygen transfer capabilities of the oxygen carriers. Models of the reactor system were developed to describe the kinetic and mass transfer phenomena taking place. It was found that the oxygen carriers could supply a cell culture of 0.2 g_{cell}/L with oxygen quickly enough such that a mass transfer limitation was not encountered. This indicated that at a minimum, the volumetric mass transfer coefficient, k_La, was equal to or greater than a value of 3 min^{-1}. This minimum value is comparable to the upper scale of performance from conventional sparging and mixing. Comparable performance was observed when using either of the two oxygen carriers.

RÉSUMÉ

Deux types de systemes transporteurs d'oxygène ont été formes: Une huile de silicone 200 cs encapsulée dans une membrane de nylon, et des micropheres solides composées d'un elastomère de silicone. La taille moyenne des particules a été 0.1 mm et 1 mm respectivement. Des cultures de cellules isolées de *Gluconobacter oxydans*, cultivées dans un milieu non-croissannt, ont été fournies d'oxygène à travers ces transporteurs. La production de DHA dans la culture a été utilisée comme le biosenseur (paramètre) pour evaluer le transfer d'oxygene. Des modèles du systeme reactionnel ont été developpés pour characteriser la cinétique et les phénomènes de transfer de masse se deroulant sur le milieu. Il a été trouvé que les transporteurs pourraient fournir oxygène à une culture cellulaire de 0.2 g_{cell}/L avec un transfert tellement rapide qu'une limitation de transfer de masse n'a pas été trouvée. Ceci indique qu'a la limite, le coefficient de tranfer de masse, k_La, a été égale ou supérieur a une valeur de 3 min^{-1}. Cette valeur minimale est comparable a celle correspondant a l'échelle superieur d'une performance dans une aeration et melange conventionel. Une performance comparable a été observée n'importe quel des deux systemes transporteurs a été utilisé.

ACKNOWLEDGEMENT

I would like to thank Dr. Neufeld for his guidance and patience, and for giving me the opportunity to perform this work. I would not have been able to solve the differential equations in this work without the help of Mehdi Rafizadeh and Francois Godin. And Mr. Dumont, who has been a pleasure to work with and a tremendous help on a daily basis for my entire time at McGill.

TABLE of CONTENTS

LIST of FIGURES

1.0 INTRODUCTION

1.1 Oxygen Transfer to Fermentations

Aerobic microorganisms need the basic requirements of: oxygen, a food source, an appropriate environment, and the removal of toxic waste products in order to survive and grow. In a fermentation, the production of biomass or metabolic products can be greatly improved by optimizing the microorganisms' immediate needs. For engineers, the financial benefits of improved performance from a fermentation are the motivation to investigate and optimize the conditions inside the reactor.

The supply of oxygen is often the limiting factor in improving the productivity of a culture. Oxygen has a very limited solubility in water (<10 mg/L), and if not replaced, would be quickly consumed by the cell culture[1]. Replenishing the dissolved oxygen is often a difficult problem, because the driving force for oxygen transfer into the liquid phase is also limited by oxygen's low solubility. This minimal buffer of available oxygen, and the ability to replenish it is the barrier that needs to be overcome in improving the productivity of an aerobic culture.

1.2 Mass Transfer Theory in a Fermenter

Oxygen dissolved in one phase must be transferred into the liquid medium where it can be available for the microorganism. Many resistances to mass transfer exist between the oxygen source and its consumer as can be seen in figure 1.

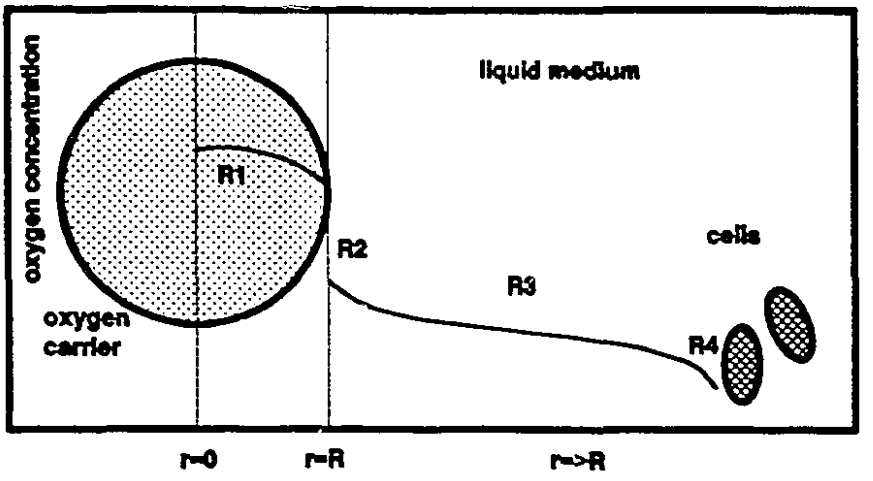

Figure 1. Schematic representation of resistances to oxygen mass transfer in an aerated fermenter.

There will be resistance to oxygen transfer through the oxygen source (R_1), at the interface (R_2), through the liquid medium (R_3) and at the surface of the microorganism (R_4). If the cells forms clumps, or are immobilized within a gel matrix then there would be yet another barrier. In a well stirred reactor, it can be assumed that both phases are well mixed and also that the interfacial resistance R_2 between the two phases is negligible[2]. The resistances to mass transfer can now be described by a series of films instead of bulk resistances, illustrated in figure 2.

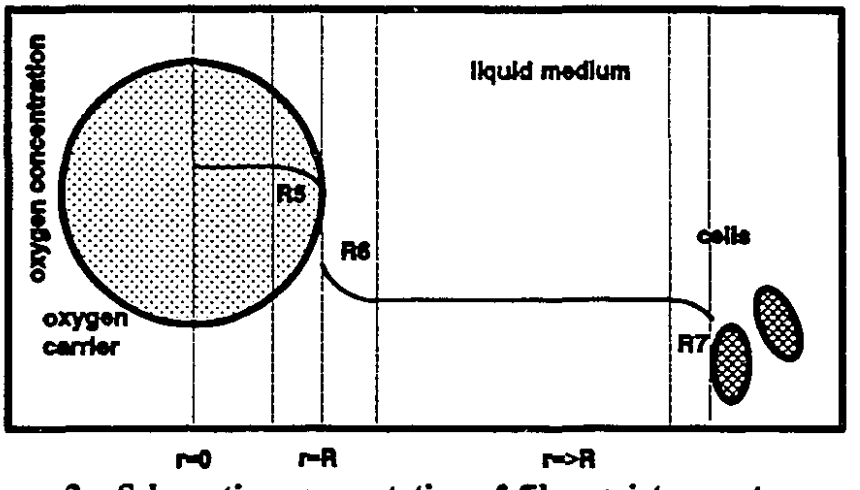

Figure 2. Schematic representation of film resistances to mass transfer in a well mixed reactor.

The properties of each film is dependant on the properties of the fluids and the level of turbulence in the reactor[3]. Films exist between the bulk oxygen phase and the interface (R5), the interface and the bulk liquid medium (R6), and the bulk liquid medium and the cell (R7). Oxygen flux through these films can be assumed to follow Fick's law of diffusion[4] stated below in equation (1). A glossary of terms and abbreviations can be found in the appendix.

$$J_A = D_{AB} \frac{dC_A}{dx} \tag{1}$$

This equation can be manipulated in the following manner to obtain the familiar form used in most bioengineering applications.

$$A * J_A = \frac{dn_A}{dt} \tag{2}$$

$$\frac{dn_A}{dt} = D_{AB} A \frac{dC_A}{dt} \tag{3}$$

$$\frac{dn_A}{dt} = \frac{dC_A V}{dt} \quad \textit{where } V \textit{ is constant} \tag{4}$$

$$\frac{dC_A}{dt} = D_{AB} \frac{A}{V} \frac{dC_A}{dx} \tag{5}$$

$$\frac{dC_A}{dx} = \frac{\Delta C_A}{\Delta x} \tag{6}$$

$$\frac{dC_A}{dt} = \left(\frac{D_{AB}}{\Delta x}\right)\left(\frac{A}{V}\right)\Delta C_A \qquad (7)$$

$$\frac{D_{AB}}{\Delta x} = k_x \qquad \frac{A}{V} = a \qquad (8)$$

Due to the difficulty in measuring the specific interfacial area between the phases, the terms k_x (most often k_L, where L represents liquid) and a are often grouped together as $k_x a$.

$$\frac{dC_A}{dt} = k_x a\ \Delta C_A \qquad (9)$$

When attempting to improve the supply of oxygen, one is usually trying to effect an improvement in one of the terms in the above equation.

1.3 Oxygen Meters and Probes

Oxygen concentration can be measured using numerous chemical, physical and electrochemical techniques. The most widespread method is the membrane covered oxygen electrode. Electrodes are measuring devices that convert the activity of a target molecule into either a voltage or a current signal. Oxygen electrodes return a current and are therefore called amperometric. In performing the measurement, the oxygen probe consumes oxygen at the surface of the cathode according to the following reaction:

$$O_2 + 2\ H_2O + 4\ e^- \rightarrow 4\ OH^- \qquad (10)$$

Therefore, eventually the oxygen conventration in the immediate environement of the probe will be lower than the bulk fluid.

The cathode surface is separated from the bulk fluid being measured by a layer of electrolyte contained within a thin oxygen permeable membrane. The consumption of the oxygen in the electrolyte causes a concentration gradient to form between the cathode and the bulk fluid, oxygen then transfers from the bulk liquid outside the membrane to the cathode's surface. At steady state, the error in the measurement associated with this flux is accommodated in the calibration of the probe. However, during transient operation, there is a lag in the instrument's output due to the delay caused by oxygen diffusion through the liquid film surrounding the surface of the probe, the membrane, and the electrolyte layer. Depending on the design of the probe, this lag can range from seconds to minutes[5]. In the event that the response lag of the probe is of the same order as the phenomenon being measured, this lag can be accounted for and the measurement corrected mathematically to avoid introducing errors in the measurement[3,6,7,13]. In the present study, it seemed inappropriate to evaluate the oxygen transfer through a nylon membrane encapsulated oxygen carrier, using a device limited by mass transfer through a teflon membrane. For this reason, a cell culture *Gluconobacter oxydans* was chosen as a "bioprobe" to measure the oxygen transfer characteristics of the microencapsulated oxygen carriers.

1.4 *Gluconobacter oxydans*

Gluconobacter oxydans (ATCC 621, other taxonomic names include *Gluconobacter suboxydans, Acetobacter suboxydans*) is a strictly aerobic, gram negative, ellipsoidal to rod shaped bacterium, approximately 1 μm in size that occurs singly and in pairs. It is a ubiquitous harmless bacteria appearing in flowers, soil, fruit, honey, beer, wine and soft drinks[8].

G. oxydans can metabolize many substrates but thrive on D-mannitol, sorbitol, and glycerol[8]. *G. oxydans* converts glycerol to dihydroxyacetone-3-phosphate (DHA3P), which then enters the pentose phosphate metabolic pathway as shown in figure 3.

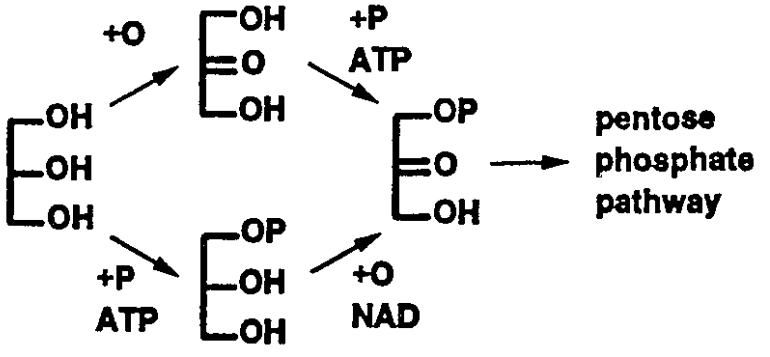

Figure 3. Metabolic pathways for the degradation of glycerol by *G. oxydans*.

There are two pathways to convert glycerol to DHA3P. In basic media glycerol is phosphorylated to glycerol-3-phosphate (GLY3P), then oxidized by an NAD dependant dehydrogenase to DHA3P. In acidic conditions, the glycerol is oxidized first into dihydroxyacetone (DHA) by a membrane linked, NAD independent glycerol dehydrogenase, then phosphorylated to DHA3P by a kinase[10,11].

The acidic media dehydrogenase is thought to shuffle the protons from the glycerol directly onto a cytochrome without the need for a NAD intermediate[63].

The acidic pathway is exploited commercially for the production of DHA because DHA is produced by the bacteria faster than it can be phosphorylated. It then accumulates in the medium where it can be recovered at the end of the fermentation[12,14]. It has been observed that the production of DHA can be decoupled from the growth of the bacteria by starting a fed batch culture with sorbitol and once enough biomass has accumulated, switching the feed to glycerol[11]. In fact, the bioconversion of glycerol to DHA can be accomplished with resting cells. This bioconversion, whether associated with growing or resting cells has a high demand for oxygen and has been used as an indicator of the oxygenation capabilities of a reactor[48].

1.5 Strategies to Improve Oxygen Supply

Various approaches have been proposed to increase the oxygen supply to the medium. Oxygen in nearly all industrial fermentations is supplied by bubble aeration. The gas film on the inside of the bubble (R_5) has negligible resistance in comparison to the exterior liquid film (R_6)[7,18,19,20]. As well, due to the small size of microbial cells, the surrounding liquid films (R_7) and corresponding concentration gradients offer negligible resistance in comparison to the liquid films surrounding the bubbles[21]. Therefore the film that controls mass transfer in a fermenter is often assumed to be the liquid film surrounding the bubbles. This is expressed as the familiar equation derived earlier in section 1.2.

$$\frac{dC_A}{dt} = k_L a * (C_{A,interface} - C_{A,bulk}) \qquad (11)$$

This equation applies to most fermentations of free cells in Newtonian broths, otherwise some of the assumptions made above and in earlier sections no longer apply.

The most common approach to increase oxygen transfer is to increase the interfacial area "a" between the two phases by increasing the turbulence in the reactor[23]. Increased turbulence also helps by reducing the film thickness around the bubble, thereby increasing the k_L term as well[23]. However, higher mixing speeds are detrimental to shear sensitive cells[25,26,27] and because it is difficult to distribute shear evenly over a large reactor[28], even in low shear environments cell death can occur near the impeller and sparger.

The driving force for mass transfer can be increased by increasing the oxygen partial pressure in the gas phase. The Deep Shaft reactor developed by DOW relies on the hydraulic head of a tall column of water to increase the total pressure and therefore the partial pressure of oxygen in the sparged bubbles as they are swept to the base of the reactor[29]. Another method of increasing the $C_{A,interface}$ term is to sparge the reactor with pure oxygen, such has been applied by Union Carbide[30]. However the cost of this method is an obvious drawback to its implementation.

In fact, the mere act of bubbling can be deleterious to shear sensitive cells. The stress that develops when bubbles break at the surface of the medium is known to rupture cells[31,32]. Reactors have been designed to alleviate this problem, but

difficulties in implementation and scale-up remain[34,35].

To eliminate mass transfer as the rate limiting step, oxygen can be generated *in-situ*. Hydrogen peroxide added to the liquid medium can be hydrolysed directly to dissolved molecular oxygen by the enzyme catalase which can either be present in the cell or added to the medium[36]. Reaction rates were observed to be many times greater with peroxide than with pure oxygen sparging, but long term exposure to peroxide was found to damage cells.

Mixed cultures of the oxygen consuming bacteria *G. oxydans* and the oxygen producing algae *Chorella pyrenoidosa* have been co-immobilized within the same gel bead. This mixed culture was found to successfully co-exist given the proper conditions and improve oxygen supply due to the symbiotic relationship between the consumer and supplier[37,38].

Attempts have also been made to remove the dependence on oxygen altogether and replace the terminal electron acceptor with another molecule. In one case p-benzoquinone was used in a culture of *G. oxydans* to convert glycerol to dihydroxyacetone as shown in figure 4.

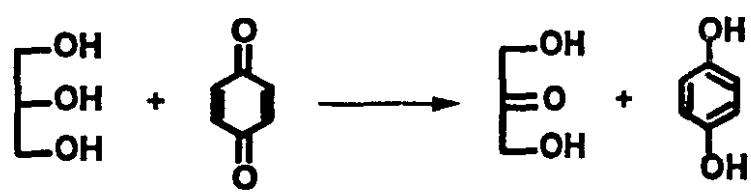

Figure 4. Conversion of glycerol to DHA using p-benzoquinone as the terminal electron acceptor instead of oxygen.

P-benzoquinone had a higher reaction rate than oxygen and is also more soluble in water giving higher overall productivities. In the process of accepting the two protons, p-benzoquinone reduces to hydroquinone and must be regenerated using hydrogen peroxide if the cycle is to be repeated. Other examples of terminal electron acceptors other than oxygen are ferricyanide and 2,6-dichloroindophenol which have been used successfully in enzymatic reactions[39,41].

The low solubility of oxygen in water makes most industrial aerobic fermentations a race to resupply what has been consumed from the medium. To increase the oxygen capacity and create a larger bank from which to draw oxygen, oxygen carriers can be added to the medium that increase the overall solubility of oxygen in the medium. Haemoglobin, hydrocarbons, and silicone and perfluorocarbon oils have been added to fermentations to increase the total mass of oxygen per liquid volume. They also indirectly improve oxygen transfer from the air phase to the liquid.

Haemoglobin is the oxygen carrying protein of red blood cells[43]. Added to the medium, haemoglobin has been shown to increase production rates in immobilized cell fermentations. Haemoglobin is most effective when cell densities are high enough to exploit the extra oxygen solvated by the added protein. Haemoglobin will slowly oxidize to met-haemoglobin which does not transport oxygen, lowering the effectiveness of this method over time. Regeneration of the met-haemoglobin or using a stabilized form of haemoglobin are possible solutions[45].

Hydrocarbons, silicone and perfluorocarbon oils are organic liquids, immiscible in water, that have a high capacity to solvate oxygen and other small

gasses, up to 20 times that in water[47,48,65,66]. The chemical structures of some of these oils are illustrated in figure 5.

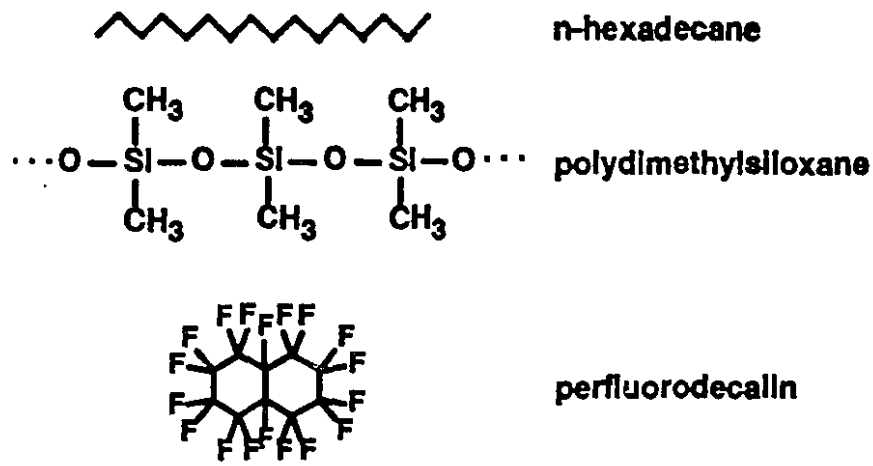

Figure 5. Chemical structure of various oxygen solvating oils.

Emulsifying these fluids into fermentation media up to 40% of the total liquid volume, then sparging with air have been shown not only to act as a buffer to oxygen depletion but also to enhance oxygen transfer[45,49,50]. It is thought that the path for mass transfer from an air bubble through the oil vector, then into the liquid offers less resistance than the direct path between the air and medium[51]. Novel reactors have been designed to take advantage of this observation and aerate a culture solely with an oxygen carrying oil. These reactors have been shown to have equivalent or better performance than convential sparging[30,52,53]. The attractiveness of this method is the fact that higher rates of oxygen transfer are possible in a comparatively low shear environment. The drawback to these methods is that certain oxygen carriers and the emulsifiers used to disperse them, have been found to be harmful to the cells being cultured[28,54,67].

To eliminate direct contact between the oxygen carrier and the cell, encapsulation of the organic phase within semi-permeable, ultra-thin, nylon membranes has been proposed and accomplished. Microencapsulated silicone oil was shown to increase the growth rate and production of a culture of *G. oxydans* in batch and continuous reactors[55].

The intent of the present study is to evaluate the oxygen transfer characteristics of encapsulated silicone oils in a batch fermentation of *G. oxydans*. The fermenter was aerated solely with oxygen carrying microcapsules containing silicone. Previously, growth of the bacteria was monitored as well as the production of DHA. In the present study only the resting cell bioconversion was monitored in a non-growth medium, the bioconversion rate was used as an indication of the oxygen that had been transferred from the oil and subsequently consumed in the reaction. Experimental data was compared to possible models describing the physical processes taking place.

2.0 OBJECTIVES

The objectives of the present study are:

-To perform and evaluate a non-growth bio-conversion of glycerol to DHA by *Gluconobacter oxydans*, using microencapsulated silicone oil oxygen carriers as the sole source of oxygen.

-To develop a model of the mass transfer taking place in the fermenter and interpret the bioconversion as an indication of the oxygen being supplied.

3.0 METHODS and MATERIALS

3.1 Growth and Maintenance of *G. oxydans*

Vials of lyophilized cultures of *G. oxydans* (ATCC 621) were obtained from the American Type Culture Collection and stored at 4°C until needed. Vials were rehydrated according to the standard instructions included with the cultures in the following medium:

glycerol (Anachemia)	50 g
yeast extract (Difco)	5.0 g
peptone (Difco)	3.0 g
NH_4Cl (Anachemia)	0.8 g
$Na_2HPO_4 \cdot 2H_2O$ (Anachemia)	0.6 g
KH_2PO_4 (Anachemia)	0.4 g
$MgSO_4 \cdot 7H_2O$ (Anachemia)	0.2 g
agar (Difco)	20 g
distilled water	up to 1 L

Rehydrated cultures were streaked onto petri dishes then transferred to agar slants. Cultures were reinoculated onto new slants every six weeks.

Cultures were prepared for experimentation in the following manner. A 250 ml erlenmeyer flask containing 100 ml of sterile medium was inoculated from a slant weekly. The seed flask was incubated on a rotary shaker a 300 rpm and 30°C for 48h, then refrigerated. 10 ml of cell suspension from the seed flask was grown in 500 ml erlenmeyer flasks containing 200 ml of medium for 18h at 300 rpm and 30°C. Aseptic technique was used in all culture transfers. Spent medium was autoclaved before disposal.

3.2 Harvesting of *G. oxydans*

Cultures were grown in 200 ml of medium inoculated using 10 ml of suspension from a seed culture stored in the fridge. After 18h incubation, the cell suspension was centrifuged at 3000 rpm for 12 minutes in a Sorvall RC5B centrifuge with a GSA head (250*g). The supernatant was decanted and 100 ml of the following buffer added.

succinic acid (Anachemia)	5.9 g
$CaOH_2$ (Anachemia)	2.8 g
distilled water	up to 1 L

The pellet was resuspended using a Vortex Geeni and washed on an orbital shaker at 200 rpm for 10 minutes. The cells were spun and washed as above a second time, then the pellet obtained was suspended in 7 ml of buffer and refrigerated.

3.3 Modified DNS Method for Quantification of Dihydroxyacetone

Dinitrosalycilic acid (DNS) reagent is a common colorimetric analytical technique used to quantify reducing sugars. Miller *et al.* (1960)[56] used a modified version of the standard DNS reagent solution to quantify carboxymethylcellulose. Modified DNS reagent was used in this work to quantify DHA. The modified reagent was prepared by combining 10 g DNS (Aldrich), 2 g phenol (Anachemia), 0.5 g Na_2SO_4 (Anachemia), 200 g potassium sodium tartrate (Rochelle salts) (Anachemia), 20 g NaOH (Anachemia), and made up to 1 L with distilled water in a volumetric flask. This solution was stored at room temperature for a maximum of 2 months.

The assay used was the following:

1. 1 ml of modified DNS reagent was added to 1 ml sample in a 16x125 mm test tube and mixed on a Vortex Geeni.
2. The sample was heated in a test tube heating block (Lab-Line) maintained at 98°C for 12 minutes.
3. The sample was cooled in running water at 15°C for 6 minutes.
4. 5 ml of distilled water was added to the sample and vortexed to mix again.
5. The absorbance of the final solution was measured in glass cuvettes (Hellma) at 575 nm in a Varian Cary 1 spectrophotometer.
6. Unknown samples were compared to a calibration curve prepared each time using known concentrations of DHA (Sigma).

3.4 Fermentation of *G. oxydans* in Batch Culture

G. oxydans was cultured to determine the optimum time for harvesting. Fermentations were carried out aseptically using a 3L benchtop fermenter (BioEngineering) filled with 3 L of growth medium. 200ml of 18h culture was used as the inoculum. The temperature was maintained at 30°C and aeration provided through a ring sparger at 3 L/min. The contents of the fermenter were mixed using two six-bladed vaned disks rotating on a magnetically driven shaft at 560 rpm. Dissolved oxygen was measured using a Cole Palmer oxygen meter (model 01971-00) with an Ingold probe. 40 ml samples of the broth were taken through a sampling port and centrifuged, the cell pellets were recovered and dried in aluminum dishes at 95°C for 24 hours to constant weight to determine cell concentrations. DHA was measured from the supernatant using the method described previously.

3.5 Microencapsulation of Silicone Oil

Microencapsulation involves forming discreet particles of fluid, confined within ultra-thin, semi-permeable membranes. For our application, silicone oils were encapsulated in polyamide nylon membranes formed by an interfacial polymerization reaction. In this reaction the monomers of the nylon are an oil soluble sebacoyl chloride and a water soluble hexanediamine. When one solution is dispersed into the other the reactive groups of the respective molecules meet at the interface and react to form a quasi-peptide bond according to the following proposed mechanism.

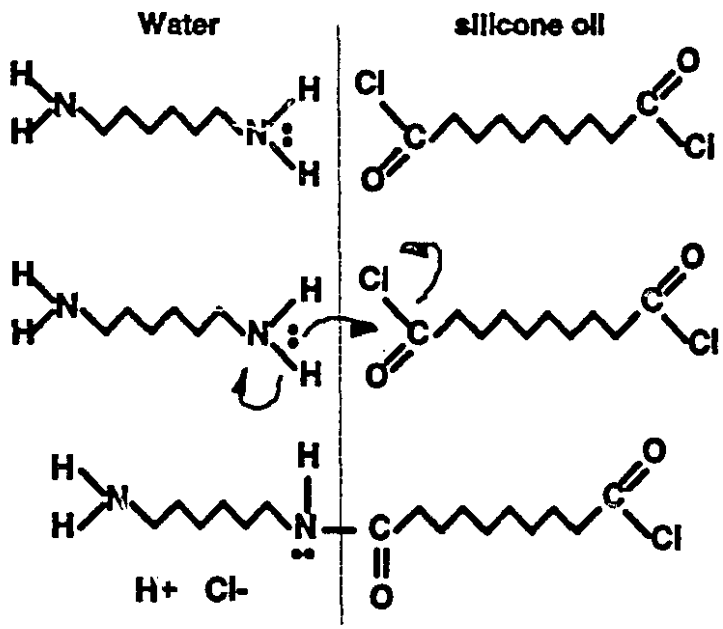

Figure 6. Mechanism for the interfacial polymerization of nylon 6,10.

Acid chloride and amine groups will continue to react and hence form long chains of nylon (in this case nylon 6,10) at the boundary between the two phases. Polyethylenimine molecules (fig. 7) cross-link the nylon chains to form the cohesive ultrathin membranes.

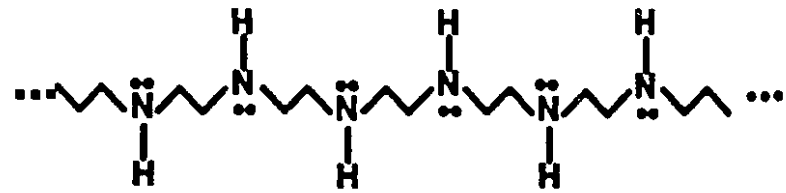

Figure 7. Chemical structure of nylon cross-linking agent polyethlenimine.

These microcapsules were developed and optimized by R. Leung and L. Centomo in previous studies[55]. The formulation conditions for the microcapsules used in the present study were those that were previously judged to provide the strongest and most robust microcapsules. The following procedure was used in preparing each batch of microcapsules.

1. The following solutions were prepared:

(i) 400 ml distilled water
8.48 g Na_2CO_3 (Anachemia) equivalent of 0.2 M
9.00 g Dow Corning 190 fluid (Dow Corning) equivalent of 2% v/v

(ii) 100 ml Dow Corning 200 cs silicone fluid (Paisley)
1.076 g sebacoyl chloride $ClOC(CH_2)_8COCl$ (Sigma) equivalent of 0.045 M

(iii) 100 ml distilled water
6.96 g hexanediamine $H_2N(CH_2)_6NH_2$ (Sigma) equivalent of 0.4 M
2.00 g 50% polyethylenimine in water solution (Sigma P-3143)
adjust the whole solution to pH 10 with HCl

(iv) 200 ml distilled water

2. In a 1 L beaker the 400 ml of buffer solution (i) was mixed with a four blade mesh screen impeller at 450 rpm.
3. The silicone oil/sebacoyl chloride solution (ii) was added and mixed for 2 minutes to form an emulsion.
4. The water/hexanediamine solution (iii) was added and mixing continued while the reaction took place for another 3 minutes.
5. 200 ml of distilled water (iv) was added to quench the reaction and mixed for an additional 2 minutes at a reduced speed.
6. The reactor contents were placed in a separatory funnel and washed and decanted with 250 ml of distilled water 5 times.

The microcapsules were stored in distilled water and gravity filtered through Whatham #4 filter paper prior to use. Particle size and distribution were measured using a Malvern (series 2600c) laser light scattering particle analyzer.

3.6 Formation of Solid Silicone Elastomer Microspheres

Experiments performed at Noranda by L. Centomo and C. Fernandez demonstrated that cured solid silicone elastomer could be used as an oxygen carrier. A process to cure silicone elastomer into solid microspheres was published by Chitambara Thanoo and Jayakrishnan[57] and then modified by Centomo and Fernandez[58]. The modifications to the recipes can be seen in the table below.

Table 1. Differences in Formulations of Solid Silicone Microspheres

	Procedure	
	Chithambara Thanoo	Centomo
Silicone elastomer	32 g	32 g
Curing agent	4.8 g	2 g
Chloroform	112 g	22 g
4% PVA continuous phase	800 g	400 g

Solid silicone elastomer microspheres were formed as follows:

1. A 4% solution of polyvinyl alcohol (PVA) MW=25000 (Polysciences INC) was prepared and allowed to cool to room temperature. The PVA acts as an emulsifying agent, other surfactants would cause the emulsion to cure as a foam rather than as discreet particles[57].
2. 32 g of MDX4-4210 room temperature vulcanizable (RTV) medical grade silicone resin (Dow Corning) was combined with 22 g of chloroform (Anachemia) and 2 g of MDX4-4210 curing agent. Air bubbles were removed from the solution using vacuum. (The MDX4-4210 products have since been replaced by the equivalent non-medical grade product Sylgard 186).

3. 400 ml of PVA solution was mixed in a 1 L beaker with a marine impeller at 500 rpm.
4. The silicone solution was slowly added to the PVA solution.
5. The temperature in the reactor was controlled using a programmable hot plate (PMC 730 Dataplate) and the beads cured according to the following temperature schedule: 2 hours at 40°C, 1 hour at 70°C, and 1 hour at 90°C. Water was added to replenish that which evaporated from the continuous phase.
6. The cured beads were allowed to cool to room temperature overnight, washed then filtered through nylon mesh and stored in distilled water.

As PVA acts as an emulsifier, it's concentration can be varied to affect the mean size of the beads, but only the beads made with the above procedure were used in the present study.

3.7 Bioconversion of Glycerol to DHA by *G. oxydans* in Non-Growth Medium

DHA production by resting *G. oxydans* was evaluated under normal bubble aeration conditions using the reactor illustrated in figure 8.

The vessel consisted of a 160 ml glass serum bottle immersed in a constant temperature bath controlled by a programmable hot plate (PMC 730 Dataplate). Compressed air was introduced through a flame constricted Pasteur pipette to improve bubble dispersion. The bottle was mixed with a 1" magnetic stir bar at 500 rpm unless noted otherwise. Air flow was held constant at 0.1 L/min, as determined using an inverted graduated cylinder.

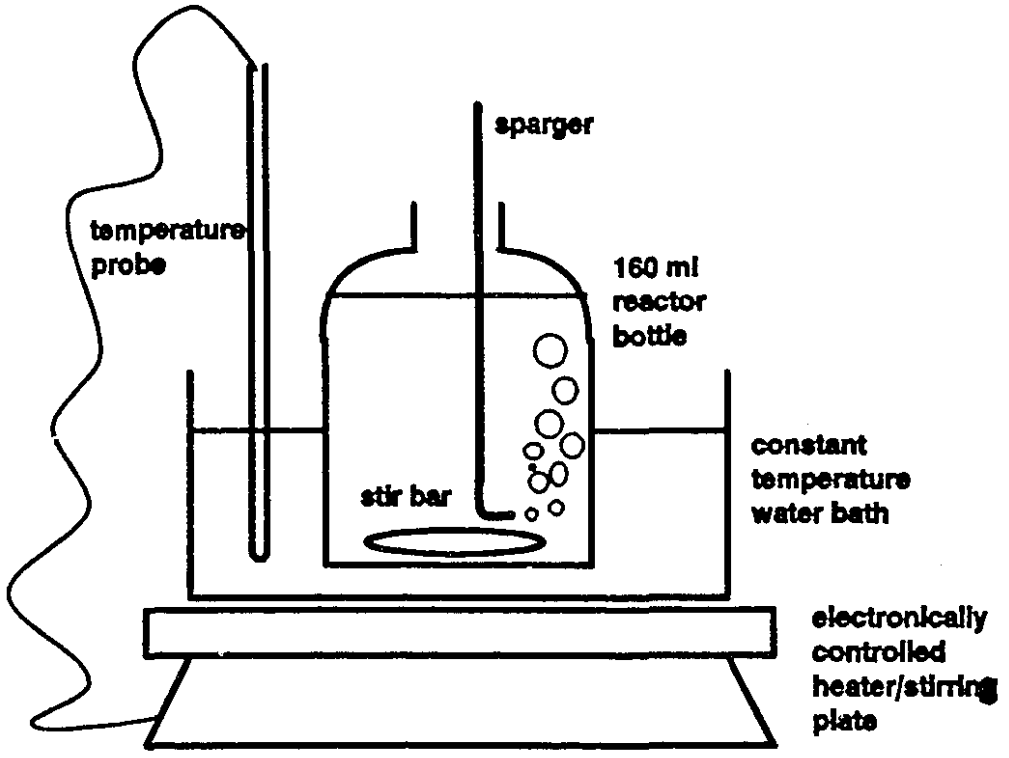

Figure 8. Schematic representation of bioconversion reactor.

The non-growth medium contained the following components.

glycerol (Anachemia)	50 g
succinic acid (Anachemia)	5.9 g
$Ca(OH)_2$ (Anachemia)	2.8 g
DHA (Sigma)	0.2 g
distilled water	up to 1 L

Succinic acid was used as the acid component of the buffer[59] and $Ca(OH)_2$ was used as the basic component in the event that Ca^{+2} alginate immobilized cells were used. DHA was added to the medium to improve its detectability by the modified DNS method in the subsequent analysis. The absence of nitrogen and phosphorous sources deprived the bacteria of the means to grow. Therefore, it was

assumed that the bioconversion of glycerol to DHA was the only oxygen consuming reaction.

The reactor was filled with 130 ml of non-growth medium and aerated for 10 minutes. 5 ml of the concentrated cell suspension (prepared as per section 3.2) stored in the fridge was warmed to 30°C in the water bath before inoculating the reactor using a micropipette.

Samples were drawn from the reactor using a 1 ml syringe and immediately vacuum filtered through a .45 μm filter (Millipore) to separate the cells from the filtrate. The filtrates were then analyzed for DHA. Temperature, mixing rate and bacteria concentration, were varied in these experiments.

3.8 Oxygen Carrier Supported DHA Bioconversion by *G. oxydans*

The reactor described above was sealed using a rubber septum, limiting the total oxygen in the reactor to the initial charge. Oxygen was supplied only from one of the following sources: an air headspace, microncapsulated silicone oil, or solid silicone microspheres.

Samples were taken in the same manner as the previous procedure except that the volume of each sample removed from the reactor was replaced by an equal volume of nitrogen gas (Matheson).

In this set of experiments the amount of oxygen carrier as well as the type of carrier was varied and all other variables were held constant.

4.0 RESULTS

4.1 Experimental Results

4.1.1 Modified DNS Method for the Quantification of DHA

DHA reacts with DNS to form an orange compound with the absorbance spectrum shown in figure 9. Measurements were taken using water in the reference cell.

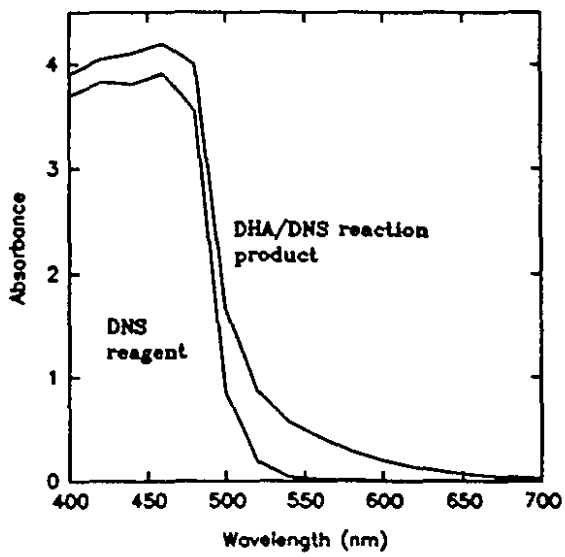

Figure 9. Absorbance spectrum of DNS and the DNS/DHA reaction product. The reference cell is water. [DHA]=0.003 mole/L

The absorbance of the DNS/DHA reaction product when measured against a reference cell containing an unreacted DNS blank has the profile illustrated in figure 10. At 575 nm, only the product of the DHA/DNS reaction absorbs light, unreacted DNS reagent absorbs at wavelengths shorter than 575 nm. Acetone, urea, succinic acid, $Ca(OH)_2$ succinate buffer and glycerol were reacted individually with modified DNS reagent. They did not contribute to the absorbance at 575 nm.

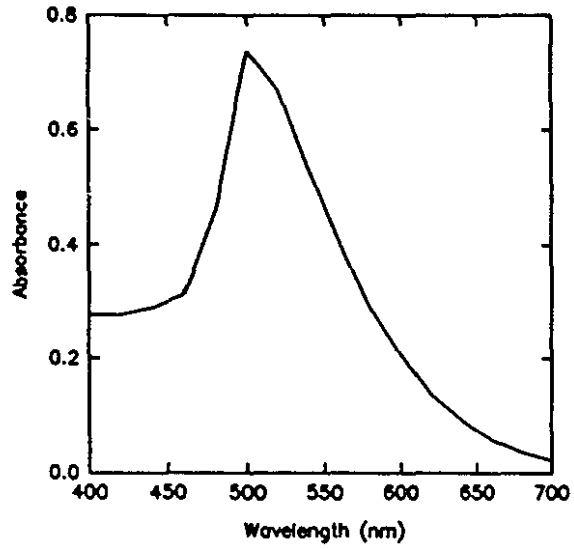

Figure 10. Absorbance spectrum of the DNS/DHA reaction product vs. a DNS blank. [DHA]=0.003 mole/L.

The calibration curves of DHA absorbance at 575 nm are presented in figures 11 and 12. The reference cell in all cases is a DHA free blank, treated in the same manner as the samples that contain DHA. From figure 11, it can be seen that a linear relationship with an absorbance less than 1 is possible in a range of DHA concentrations less than 0.010 mole/L. The following linear relationship is obtained when a regression is performed and the line is not forced through the origin. These values were obtained consistently over the duration of the project.

$ABS = 113.3 * [DHA] - 0.045 \qquad R^2 = 0.998 \qquad$ units are (mole/L)

The detection limit of the assay of approximately 0.0012 mole/L of DHA can be seen in the plot at low DHA concentrations (fig. 12).

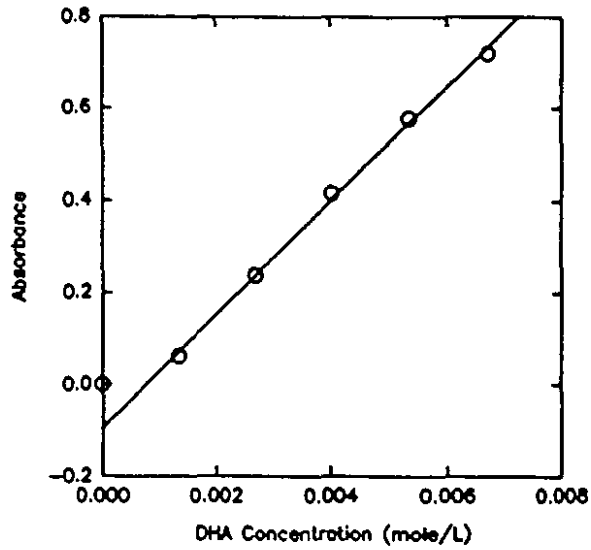

Figure 11. Linear portion of plot of Absorbance vs. DHA concentration.

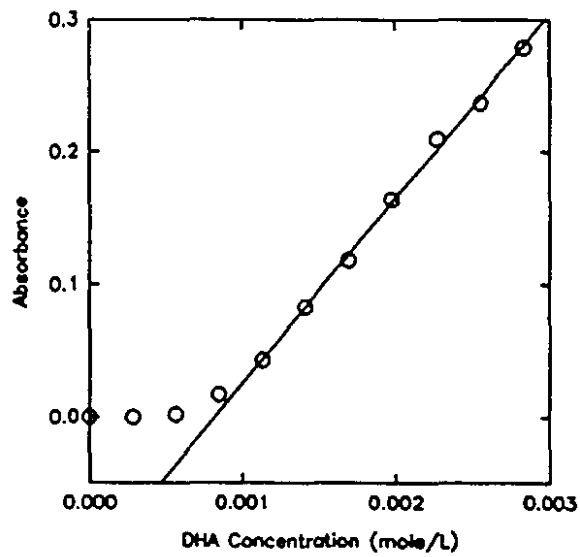

Figure 12. Low concentration profile of absorbance vs. DHA concentration.

4.1.2 Dryweight Estimation of *G. oxydans* by Absorbance Measurement

The absorbance spectrum of *G. oxydans* suspended in Ca-succinate buffer is shown in figure 13. The reference is cell free buffer.

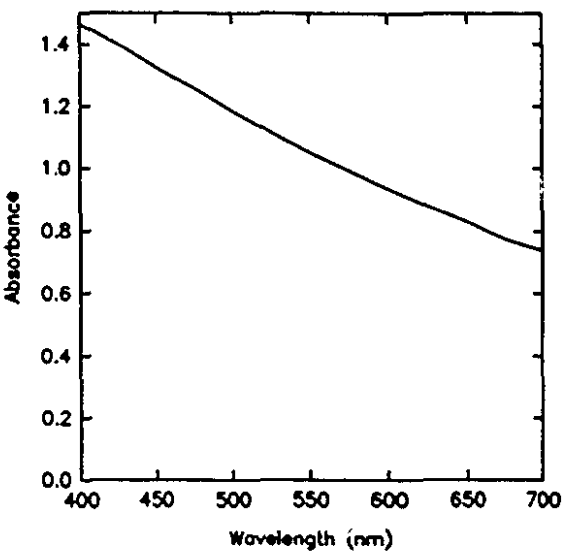

Figure 13. Absorbance spectrum of *G. oxydans* suspended in buffer against a reference cell of cell free buffer.

The calibration curve of absorbance vs. cell concentration was taken at 575 nm and is presented in figure 14.

A linear regression was forced through the origin and the following relationship obtained.

$ABS = 2.45 * [cell]$ $\quad R^2 = .994$ $\quad$ units are (g/L) dryweight

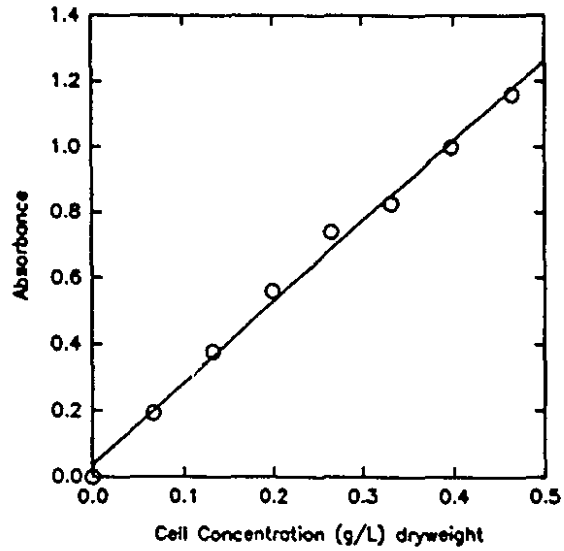

Figure 14. Calibration curve of absorbance vs. concentration of cells suspended in buffer.

4.1.3 Growth of *G. oxydans* in Batch Culture

G. oxydans was cultured on glycerol growth medium. Cell dryweight, DHA production and dissolved oxygen levels were monitored as shown in figure 15 and 16.

It can be seen in figure 15 that dissolved oxygen levels rapidly approach zero as the ability to supply oxygen to the culture is taxed. The culture continues to grow rapidly (fig. 16) and produce DHA even at low oxygen concentrations. The culture is in the exponential growth phase at 18 hours and is still highly active, biomass is approximately three quarters of the maximum possible. Harvesting at this point in the fermentation would provide a high recovery of the most active cells.

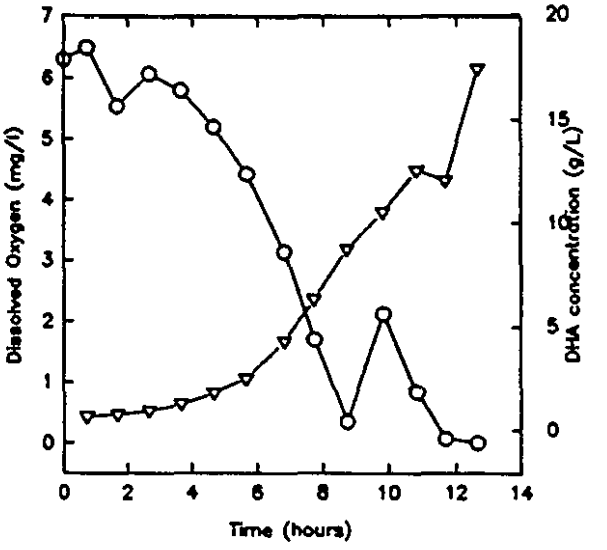

Figure 15. Batch fermentation of *G. oxydans* on glycerol growth medium. DHA (▽) and dissolved oxygen (O) were monitored with time.

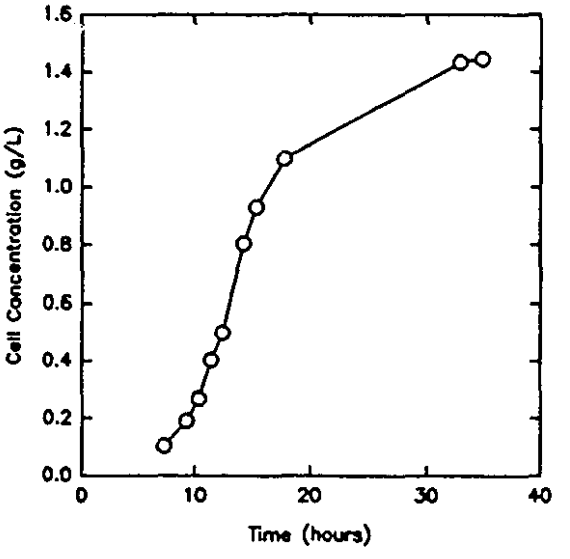

Figure 16. Batch growth of *G. oxydans* on glycerol growth medium.

4.1.4 Formation of Silicone Oil Microcapsules

The nylon membrane encapsulation procedure formed discreet spherical microcapsules. A small amount of non-encapsulated oil was observed floating above the washed microcapsules, and some nylon membrane breakage was noted microscopically. Fresh reagents reduced the extent of oil loss due to membrane breakage. The size distribution of the resulting microcapsules is illustrated in figure 17.

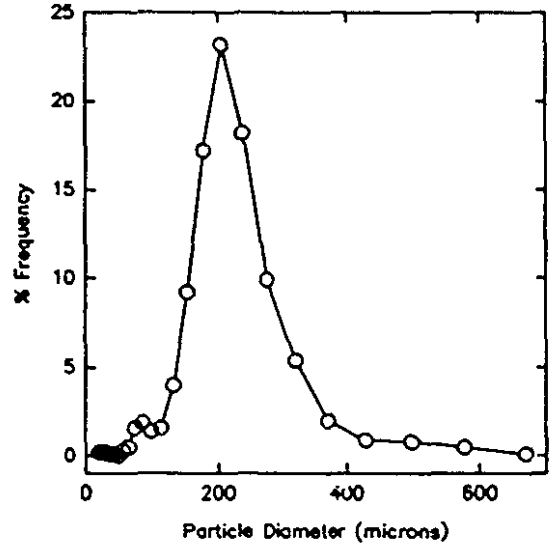

Figure 17. Size distribution of nylon encapsulated silicone oil microcapsules

The deSauter mean particle diameter (d_{32}) was 137.7 μm, and the specific surface area was 39,300 m^2/m^3.

4.1.5 Formation of Solid Silicone Elastomer Microspheres

The microspheres formed using the technique modified by Centomo and Fernandez were discreet and spherical. Approximately 80% of the original mass of silicone elastomer could be recovered as discreet beads while the rest was agglomerated to the impeller and reactor. The size distribution as determined by the Malvern particle sizer can be seen in figure 18.

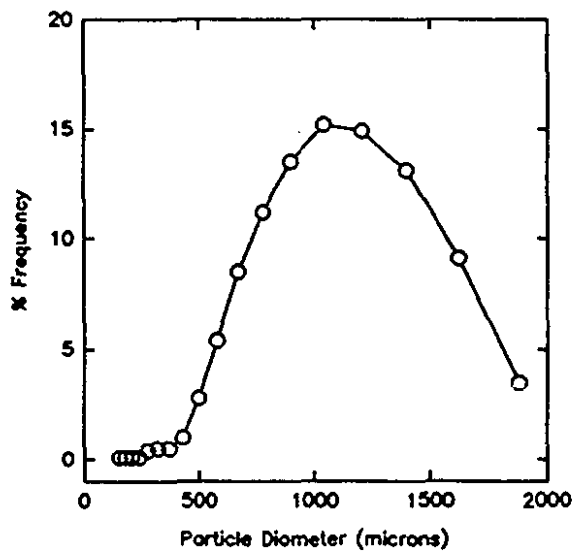

Figure 18. Size distribution of solid silicone elastomer microspheres.

The mean diameter of the microspheres was d_{32}=837.4 μm and the specific surface area 6900 m^2/m^3.

4.1.6 Non-Growth Production of DHA with Varied Cell Concentration

The DHA production rate was determined on non-growth medium containing glycerol, at various cell inoculum levels. Fermentations were carried out as described earlier and the rates of DHA production are plotted in figures 19 and 20. The rates of production in both plots can be seen to be higher with increased innoculum level. The production rates of each run are tabulated in table 2. The specific production rates based on a per gram of cell dryweight basis are calculated and included in the same table. It can be seen that the specific productivity is constant at approximately 1e-3 (mole DHA/g_{cell}*L).

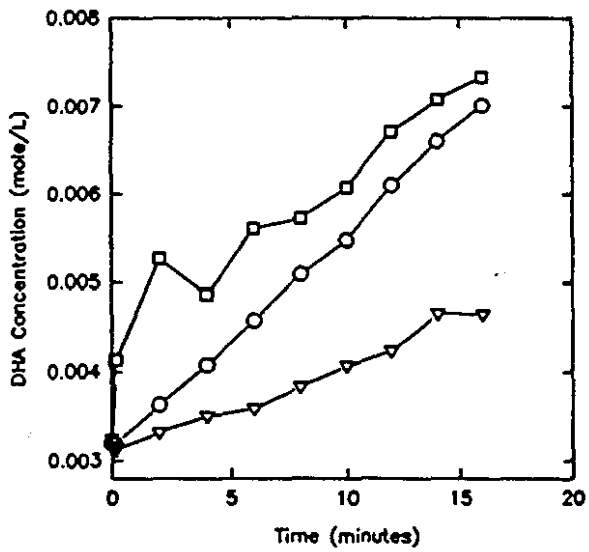

Figure 19. DHA produced by resting *G. oxydans* at 0.58 (□), 0.17 (○), 0.06 (▽) g/L dryweight of cell innoculum.

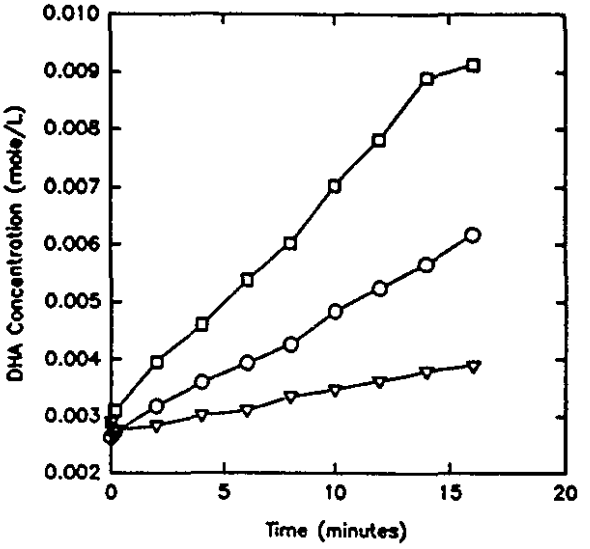

Figure 20. DHA produced by resting *G. oxydans* at 0.48 (□), 0.14 (○), 0.05 (▽) g/L dryweight of cell innoculum.

Table 2. DHA Production Rates Under Varied Cell Loading

cell concentration (g dryweight/L)	activity (mole DHA/ min*L)	specific activity (mole DHA/ g cell*L)
0.05	0.71e-4	1.55e-3
0.06	0.99e-4	1.70e-3
0.14	2.16e-4	1.57e-3
0.17	2.42e-4	1.39e-3
0.48	3.98e-4	0.83e-3
0.58	2.43e-4	0.42e-3

4.1.7 Non-Growth Production of DHA Under Varied Mixing Conditions

The dependance of DHA production on the mixing rate can be seen in figures 21 and 22.

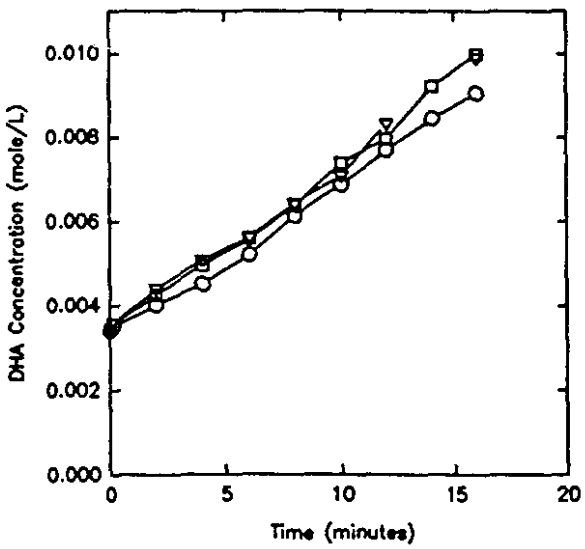

Figure 21. DHA produced by *G. oxydans* on non-growth medium at 100 (▽), 400 (○), and 700 (□) rpm mixing rate. Cell loading was 0.23 g/L.

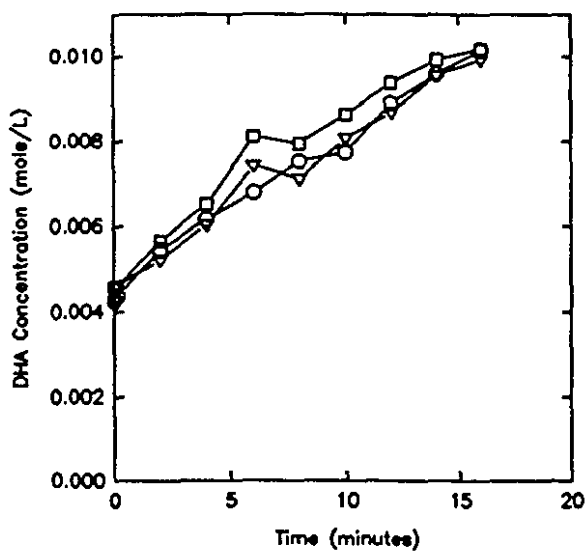

Figure 22. DHA produced by *G. oxydans* on non-growth medium at 0 (▽), 100 (○), 300 (□) rpm mixing rate. Cell loading was 0.29 g/L.

It is apparent in the plots that the rate of production is not affected by the stirrer speed in the reactor. Had mass transfer resistance been a factor in determining the rate of appearance of DHA then some change due to mixing speed should have been observed. The rates as determined by linear regression are presented in table 3. The specific activity of the cells has been calculated and included in the table. Once again it is apparent that the culture has a specific activity of approximately 1e-3 (mole DHA/g_{cell}*L).

Table 3. DHA Production Under Varied Mixing Conditions

mixing rate	cell concentration	activity	specific activity
rpm	g dryweight/L	mole DHA/ (L*min)	mole DHA/ (g cell * min)
0	0.29	3.60e-4	1.23e-3
100	0.23	4.03e-4	1.79e-3
100	0.29	3.60e-4	1.23e-3
300	0.29	3.48e-4	1.18e-3
400	0.23	3.61e-4	1.60e-4
700	0.23	3.96e-4	1.76e-3

4.1.8 Non-Growth Production of DHA Under Varied Fermenter Temperature

DHA production at various temperatures is illustrated in figure 23.

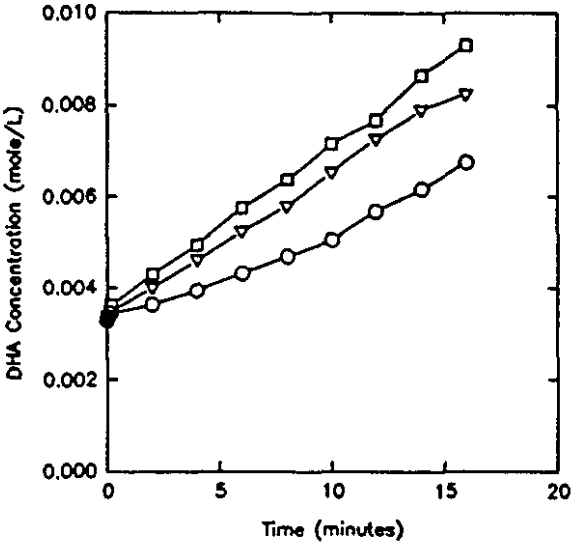

Figure 23. DHA produced by *G. oxydans* on non-growth medium at 24.5 (○), 30 (▽), 35.5°C (□). Cell loading was 0.26 g/L.

The rate of DHA production can be seen to increase as the temperature in the fermenter is increased. The rates as determined by linear regression are presented in table 4. It can be seen in the calculated relative activities included in the table that the activity of the culture has almost doubled over a temperature range of 10°C.

Table 4. DHA production Rates at Various Temperatures

temperature (°C)	activity (mole DHA/L*min)	relative activity
24.5	3.62e-4	1.14
30.0	3.17e-4	1.0
35.5	2.08e-4	0.66

4.1.9 Non-growth Production of DHA Varying the Loading of Oxygen Carriers

The loading of microencapsulated silicone oil was varied in the following set of experiments. The ratios of silicone oil to liquid medium to cell innoculum are illustrated schematically in figure 24.

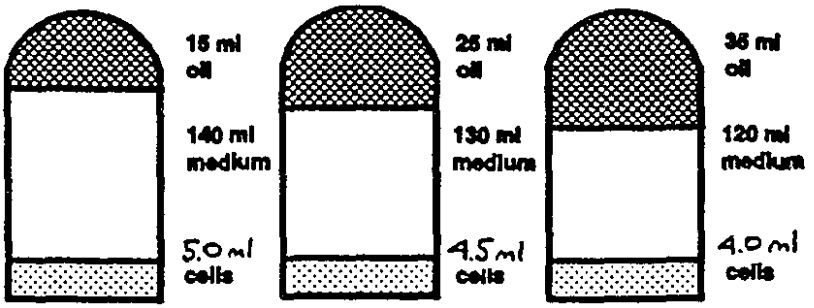

Figure 24. Schematic representation of varying the silicone oil microcapsule loading of the reactor.

The amount of oxygen available was limited to that which was initially dissolved in the microcapsules and the liquid medium at the start of the experiment. It can be observed in figures 25 and 26 that the rates of DHA production are similar to approximately 3 minutes when the rates diverge due to the differences in oxygen carrier loading.

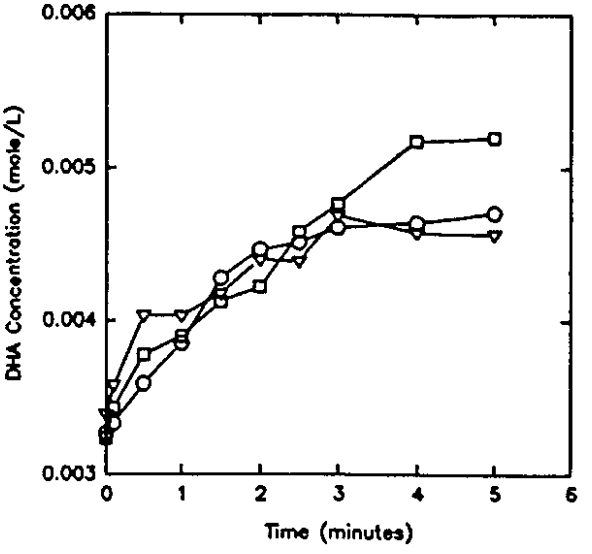

Figure 25. DHA produced by *G. oxydans* in non-growth medium with 15 (▽), 25 (○), 35 (□) ml of silicone oil microcapsules. Cell loading was 0.3 (g cell/L).

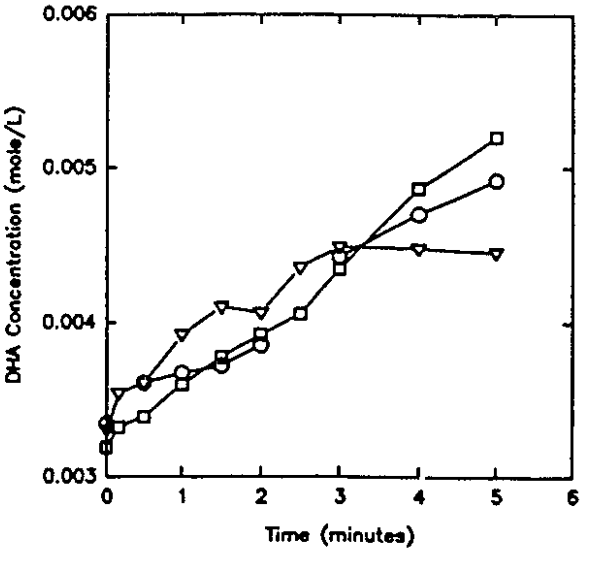

Figure 26. DHA produced by *G. oxydans* in non-growth medium with 15 (▽), 25 (○), and 35 (□) ml of silicone oil microcapsules. Cell loading was 0.24 (g cell/L).

4.1.10 Non-Growth Production of DHA Using Different Oxygen Carriers.

The oxygen carrier was varied by using equal volumes of one of the following carriers of oxygen: air headspace, microencapsulated silicone oil and solid silicone microspheres. All other conditions of the fermentation were the same as the other closed system fermentations. The production of DHA can be seen in figure 27.

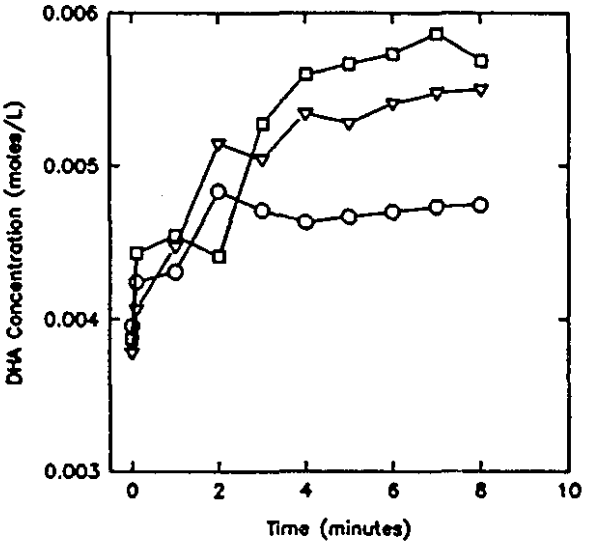

Figure 27. DHA produced by *G. oxydans* on non-growth medium supplemented with: 25 ml silicone oil microcapsules (□), 25 ml solid silicone microspheres (▽), 25 ml air (○). Cell loading was 0.3 g cell/L.

From figure 27 the production of DHA can be seen to be best for the microencapsulated silicone oil, followed by the solid silicone microspheres and lastly the air headspace.

4.2 Modelling of the Non-Growth Production of DHA

Models were developed to describe the oxygen transfer behaviour of the microencapsulated silicone oil. Comparisons to the experimental results will highlight the significance of the various mass transfer phenomena.

The models all share the following characteristics and assumptions. The system contains a fixed volume of 100 μm diameter silicone oil microcapsules. Due to the small size, oil viscosity, and polymer coating, the microcapsules are considered to be rigid spheres with no internal mixing. The oxygen content of oxygen saturated silicone oil in equilibrium with air is $C_{O2S\phi}$=6.25 mmole O_2/L[66]. The ultra thin nylon membrane is assumed to have no resistance to mass transfer. The oxygen carriers are suspended in a perfectly-mixed medium where glycerol is available in excess. There is an initial background level of DHA in the reactor equal to 3.33 mmole/L corresponding to the background level used in the experimental medium. The diffusivity of oxygen in silicone oil is 2.2e-9 m^2/s [68]. Dissolved oxygen at the interface between the silicone oil and liquid medium is assumed to be in thermodynamic equilibrium according to the following Henry's law relationship $C_{O2Si}=H*C_{O2Li}$, where H=20 [65]. Surrounding each bead is a liquid film with an associated resistance to mass transfer. Bacteria are evenly distributed in the liquid medium, and the liquid film surrounding each cell is considered negligible. The cells consume oxygen at a rate described by Michealis-Menten kinetics, where oxygen is the limiting substrate[40].

$$\frac{dC_{DHA}}{dt} = \frac{k * b * C_{O2L}}{K_m + C_{O2L}} \qquad (12)$$

The appearance of DHA in the liquid medium can be related to the depletion of O_2 from the microcapsules according to the stoichiometric relationship.

$$2\ Glycerol + O_2 \rightarrow 2\ DHA + 2\ H_2O \qquad (13)$$

For the purposes of modelling, the system was split into three locations. These locations are: the mass transfer in the interior of the microencapsulated silicone oil, the mass tranfer on the exterior of the microcapsule, and the reaction at the cell surface. At each location, two different approaches to model the behaviour of oxygen at that point were considered. These can be seen in table 5.

Table 5. Mathematical Descriptions of Oxygen Behaviour at Three Locations in the Reactor

	LOCATION		
	Mass transfer inside O_2 carrier	Mass transfer outside O_2 carrier	Reaction at the cell surface
Oxygen behaviour modelled as	no resistance i.e. lumped capacitance	no resistance	zero order, very fast reaction rate for all $[O_2]$
	resistance to diffusion due to spatial effects	liquid film resistance	Michealis-Menten kinetics

At each of the three locations, one of the two oxygen behaviors listed in that column was chosen. The different permutations of these choices gives rise to the following four models.

-Kinetic Limitation model
-Liquid Film Mass Transfer Resistance model
-Combination Liquid Film Resistance and Kinetic Limitation model
-Combination Internal and Liquid Film Mass Transfer Resistance model

The following nomenclature will be used for the models:

n	moles	-with subscipts	(moles)
C	concentration	-with subscripts	(mole/L)
-subscripts	species:	**O2** -oxygen, **D** -DHA	
	phase:	**S** -silicone, **L** -liquid, **T** -total	
	other:	**i** -interface, **ϕ** -time zero	

V	volume (L)
E	reaction extent i.e. number of moles reacted (moles)
r	radial position inside microcapsule (m)
R	microcapsule radius (m)
a	specific area (m^2/m^3)
H	Henry's constant
k	rate constant (mole/ g_{cell}*min)
b	cell inoculum (g_{cell}/L)
K_m	Michealis constant (mole/L)
k_La	liquid film mass transfer coefficient (min^{-1})
D_{O2S}	diffusivity of O_2 in silicone oil (m^2/min)
t	time (min)

4.2.1 Kinetic Limitation Model

In the Kinetic Limitation model, it is assumed that the rate of DHA production is kinetically controlled. Oxygen mass transfer in the microcapsule and in the liquid film is assumed to be instantaneous. A schematic of these assumptions is illustrated in figure 28.

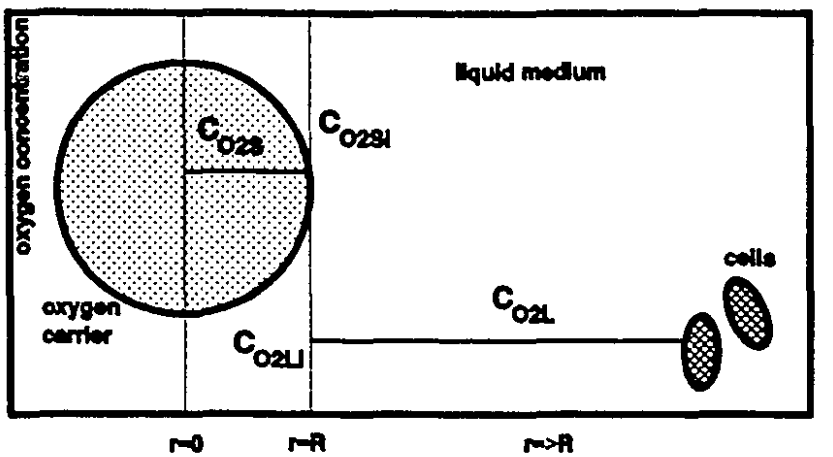

Figure 28. Schematic representation of the Kinetic Limitation model system.

From the stoichiometry, an expression for the liquid phase concentration of oxygen in terms of measurable quantities is obtained.

$$O_2 \rightarrow 2\ DHA \tag{14}$$

The stoichiometric table is therefore.

$$n_{DL} = n_{DL\phi} + 2\ E \tag{15}$$

$$n_{O2T} = n_{O2S\phi} + n_{O2L\phi} - E \tag{16}$$

The total oxygen in the system is the sum of what is contained in the two phases.

$$n_{O2T} = n_{O2S} + n_{O2L} \tag{17}$$

Replacing (17) into (16) and then converting the stoichiometric table to concentration terms gives.

$$C_{DL} * V_L = C_{DL\phi} * V_L + 2E \tag{18}$$

$$C_{O2S}*V_S + C_{O2L}*V_L - C_{O2S\phi}*V_S + C_{O2L\phi}*V_L - E \quad (19)$$

Equate the reaction extents in equations (18) and (19) to eliminate E.

$$2*[C_{O2S\phi}*V_S + C_{O2L\phi}*V_L - C_{O2S}*V_S - C_{O2L}*V_L] - C_{DL}*V_L - C_{DL\phi}*V_L \quad (20)$$

Using Henry's law, replace silicone $[O_2]$ with liquid $[O_2]$ in equation (20).

$$C_{O2S} = H * C_{O2L} \quad and \quad C_{O2S\phi} = H * C_{O2L\phi} \quad (21)$$

$$2*[H*C_{O2L\phi}*V_S + C_{O2L\phi}*V_L - H*C_{O2L}*V_S - C_{O2L}*V_L] - C_{DL}*V_L - C_{DL\phi}*V_L \quad (22)$$

Collect like terms and isolate C_{O2L}.

$$C_{O2L} = \frac{2*C_{O2L\phi}*(H*V_S+V_L) - V_L*(C_{DL}-C_{DL\phi})}{2*(H*V_S+V_L)} \quad (23)$$

Replace the expression for C_{O2L} into the following kinetic relationship

$$\frac{dC_{DL}}{dt} = \frac{k * b * C_{O2L}}{K_m + C_{O2L}} \quad (24)$$

$$\frac{dC_{DL}}{dt} = \frac{k * b * \left(\frac{2*C_{O2L\phi}*(H*V_S+V_L) - V_L*(C_{DL}-C_{DL\phi})}{2*(H*V_S+V_L)}\right)}{K_m + \left(\frac{2*C_{O2L\phi}*(H*V_S+V_L) - V_L*(C_{DL}-C_{DL\phi})}{2*(H*V_S+V_L)}\right)} \quad (25)$$

For the solution above, the following numerical values were used and the results of the model, solved using MATLAB, are plotted in figures 29 and 30. The MATLAB programs are included in the appendix.

k=	1.24e-3 mole DHA/(g_{cell}*min)
b=	from 0.1 to 0.4 variable
K_m=	8.6e-6 mole O_2/L
$C_{O2L\phi}$=	3.1e-3 mole O_2/L
$C_{DL\phi}$=	3.3e-3 mole DHA/L
H=	20
V_S=	from .015 to .035 L
V_L=	from .125 to .145 L

It can be seen in figure 29 that DHA accumulates in the liquid medium at a constant rate until the end of the fermentation. The rate of DHA production is relatively independant of the concentration of oxygen in the liquid phase which is slowly decreasing as it is being consumed. The final amount of DHA produced during the fermentation is determined by the initial amount of dissolved oxygen contained in the microcapsules. In figure 30 it can be seen that the rate of DHA production is determined by the innoculum level.

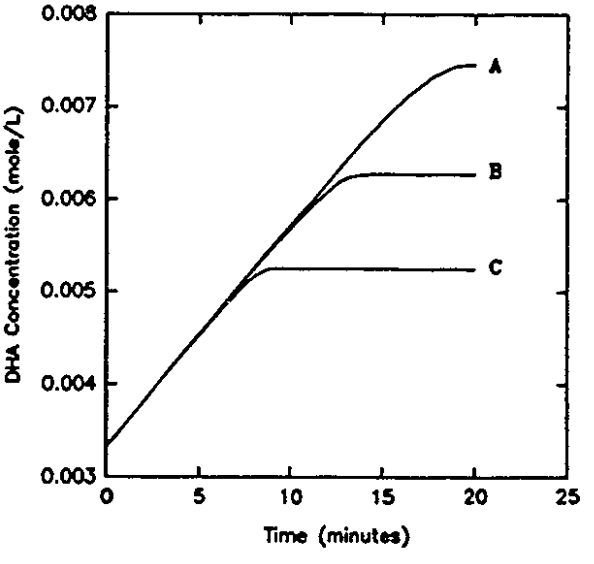

Figure 29. Model predictions of DHA produced by *G. oxydans* in non-growth medium with 15 (C), 25 (B), 35 (A) ml microencapsulated silicone oil. Cell loading was 0.2 g/L

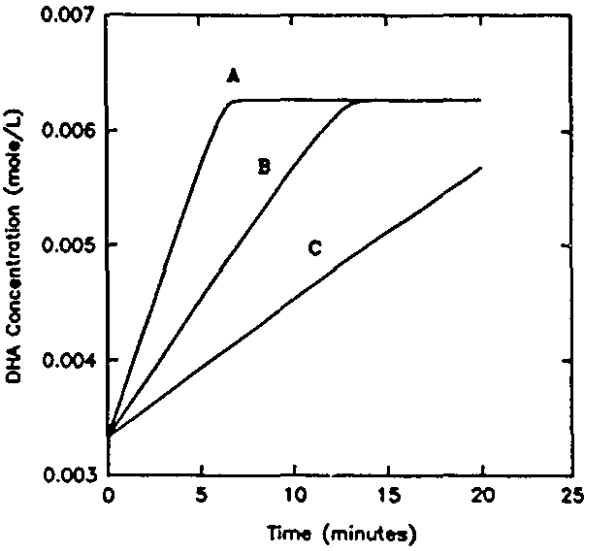

Figure 30. Model predictions of DHA produced by *G. oxydans* in non-growth medium with 0.1 (C), 0.2 (B), 0.4 (A) g cell/L. oil volume constant at 25 ml.

4.2.2 Liquid Film Mass Transfer Resistance Model

In the following model, oxygen diffusion through the liquid film surrounding the silicone oil microcapsules is assumed to be the rate limiting step in the conversion of oxygen to DHA. There is no radial concentration gradient of oxygen inside the microcapsules. The culture produces DHA at a very fast rate at all concentrations of oxygen, therefore as soon as a molecule of oxygen crosses the liquid film it appears in the medium as DHA. The concentration of oxygen in the liquid medium is therefore assumed to be zero. A schematic of the model system can be seen in figure 31.

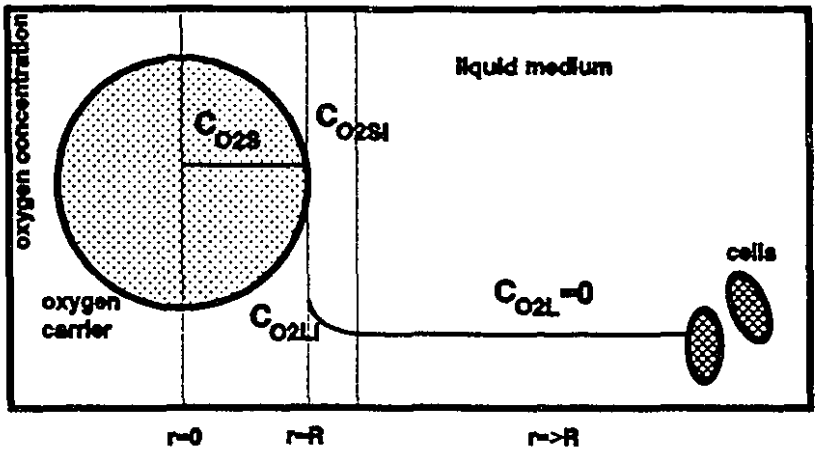

Figure 31. Schematic representation of Liquid Film Mass Transfer Resistance model system.

The mass transfer through a liquid film can be described by the following equation derived in section 1.2.

$$\frac{dC_{O2S}}{dt} = -k_L a * (C_{O2Li} - C_{O2L}) \tag{26}$$

Assuming that the oxygen concentration in the liquid phase is zero.

$$C_{O2L} = 0$$
$$\frac{dC_{O2S}}{dt} = -k_L a * (C_{O2Li}) \tag{27}$$

Replace C_{O2Li} using Henry's law.

$$C_{O2Si} = H * C_{O2Li}$$
$$\frac{dC_{O2S}}{dt} = -k_L a * \left(\frac{C_{O2Si}}{H}\right) \tag{28}$$

The lumped capacitance assumption is used to replace C_{O2Si} in equation (28).

$$\frac{\partial C_{O2S}}{\partial r} = 0 \quad \therefore \quad C_{O2Si} = C_{O2S}$$
$$\frac{dC_{O2S}}{dt} = -k_L a * \left(\frac{C_{O2S}}{H}\right) \tag{29}$$

The differential equation in (29) is intergrated with the following initial condition.

$$\textit{initial condition @ } t=0 \quad C_{O2S}=C_{O2S\phi}$$
$$\int_{C_{O2S\phi}}^{C_{O2S}} \frac{dC_{O2S}}{C_{O2S}} = \frac{-k_L a}{H} \int_0^t dt \tag{30}$$

$$\ln\left(\frac{C_{O2S}}{C_{O2S\phi}}\right) = \frac{-k_L a}{H} * t \tag{31}$$

From the stoichiometry the disappearance of O_2 can be replaced with the appearance of DHA in the following manner.

$$O_2 \rightarrow 2\ DHA \tag{32}$$

The stoichiometric table is therefore.

$$n_{DL} = n_{DL\phi} + 2\ E \tag{33}$$

$$n_{O2S} = n_{O2S\phi} - E \tag{34}$$

Convert equations (33) and (34) to concentration terms.

$$C_{DL}*V_L = C_{DL\phi}*V_L + 2\ E \tag{35}$$

$$C_{O2S}*V_S = C_{O2S\phi}*V_S - E \tag{36}$$

Equate the reaction extents in equation (35) and (36) to eliminate E and isolate C_{O2S}.

$$C_{O2S} = C_{O2S\phi} - \frac{V_L}{2*V_S}*(C_{DL}-C_{DL\phi}) \tag{37}$$

Replace C_{O2S} in equation (31) with the expression from equation (37) to obtain.

$$\ln\frac{\left(C_{O2S\phi}-\frac{V_L}{2*V_S}*(C_{DL}-C_{DL\phi})\right)}{C_{O2S\phi}} = \frac{-k_La}{H}*t \tag{38}$$

Collect like terms and isolate C_{DL} to obtain an expression relating DHA concentration to time.

$$C_{DL} = C_{DL\phi} + \frac{2*V_S}{V_L}*C_{O2S\phi}*\left(1-\exp\left(\frac{-k_La}{H}*t\right)\right) \tag{39}$$

For the solution above, the following numerical values were used and the results of the model are plotted in figure 32 and 33.

$C_{O2S\phi}$=	6.3e-3 mole O_2/L
$C_{O2L\phi}$=	0.0 mole O_2/L
$C_{DL\phi}$=	3.3e-3 mole DHA/L
H=	20
V_S=	from .015 to .035 L
V_L=	from .125 to .145 L
k_La=	variable

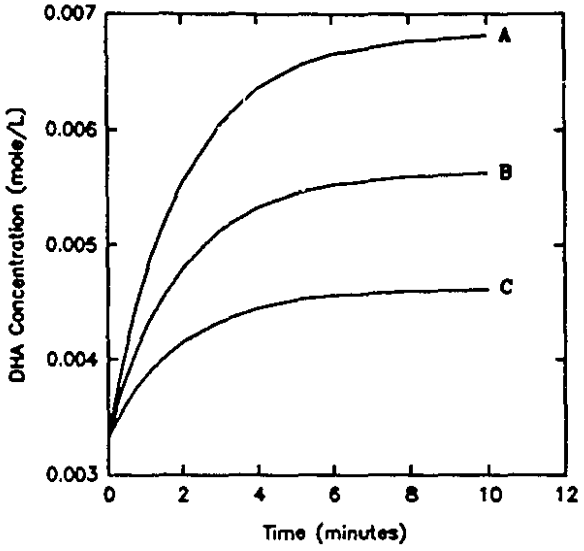

Figure 32. Model predictions of DHA produced by *G. oxydans* on non-growth medium with 15 (C), 25 (B), 35 (A) ml of silicone microcapsules. k_La is constant at 10.0 min^{-1}.

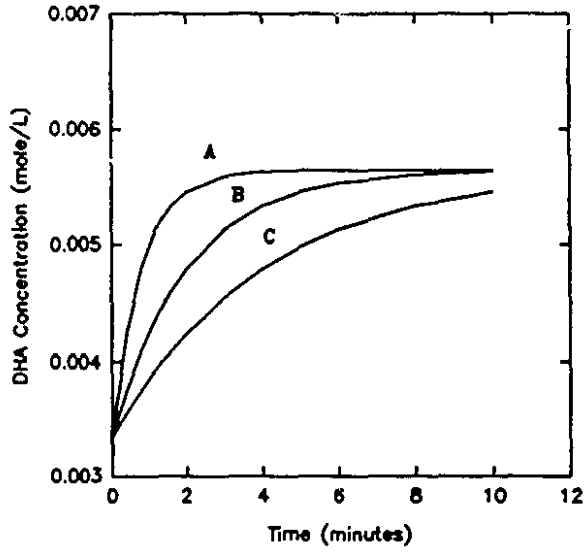

Figure 33. Model predictions of DHA produced by *G. oxydans* on non-growth medium at k_La equal to 5 (C), 10 (B), 25 (A) min^{-1}. Oil volume is 25 ml.

It can be seen in figure 32 that the concentration of DHA rises to the final equilibrium value in an exponential decay. The final amount of DHA produced during the fermentation is determined by the initial charge of oxygen contained in the microcapsules. In figure 33 one can observe that as the value of k_La is increased the steepness of the exponential rise is also increased.

4.2.3 Combination Liquid Film Resistance and Kinetic Limitation Model

The following model assumes that both the film resistance and kinetic limitation to the consumption of oxygen are both taking place. At the start of the experiment, the silicone and liquid phases are saturated with oxygen. The cells are introduced to the reactor at time zero. The cells consume the oxygen in the liquid phase at a rate dependant on its concentration. This disappearance of oxygen from the liquid medium causes new oxygen to transfer into the liquid medium from the microcapsules at a rate dependant on the concentration gradient. These events are coupled, and lead to the following model which is a solution of two simultaneous differential equations. A schematic representation of the model is presented in figure 26.

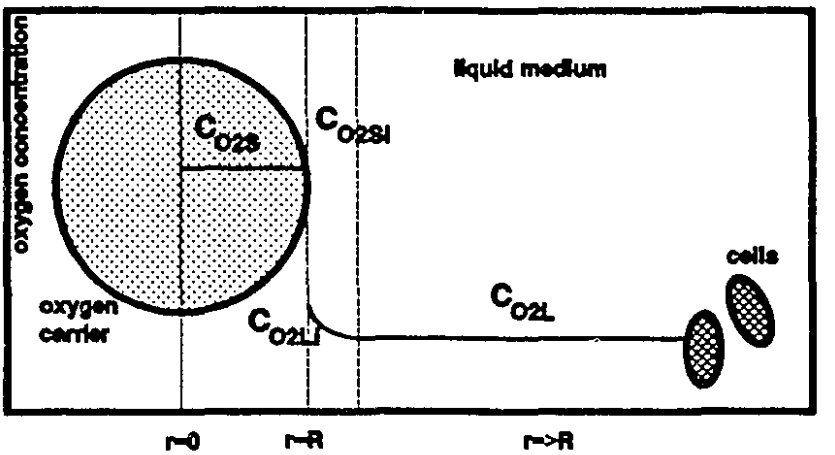

Figure 34. Schematic representation of Combination Liquid Film Resistance and Kinetic Limitation model system.

First an expression for the rate of change of oxygen concentration in the silicone microcapsule phase is obtained. Starting with a mass balance on oxygen around silicone microcapsule phase.

$$\textit{Accumulation} = \textit{input} - \textit{output} + \textit{generation}$$

$$\left(\frac{dC_{O2S}}{dt}\right)_{total} = 0 - \left(\frac{dC_{O2S}}{dt}\right)_{m.t.} + 0 \tag{40}$$

Mass transfer (m.t.) from the silicone phase is described as the following equation derived earlier in section 1.2.

$$\left(\frac{dC_{O2S}}{dt}\right)_{m.t.} = -k_L a*(C_{O2Li}-C_{O2L}) \tag{41}$$

Using the Henry's law relationship and the lumped capacitance assumption C_{O2Li} is replaced with C_{O2S}.

$$C_{O2Si} = H * C_{O2Li} \quad \textit{and} \quad C_{O2S} = C_{O2Si} \tag{42}$$

$$\left(\frac{dC_{O2S}}{dt}\right)_{total} = -k_L a * \left(\frac{C_{O2S}}{H} - C_{O2L}\right) \tag{43}$$

The rate of change of oxygen concentration in the liquid phase is obtained by starting with a mass balance on oxygen around the liquid phase.

$$Accumulation = input - output + generation$$

$$\left(\frac{dC_{O2L}}{dt}\right)_{total} = \left(\frac{dC_{O2L}}{dt}\right)_{m.t.} - 0 + \left(\frac{dC_{O2L}}{dt}\right)_{reaction} \tag{44}$$

The moles of oxygen that are leaving the silicone phase are equal to the moles that are entering the liquid phase, therefore.

$$\left(\frac{dn_{O2S}}{dt}\right)_{m.t.} = -\left(\frac{dn_{O2L}}{dt}\right)_{m.t.} \tag{45}$$

Converting equation (45) to concentration terms gives.

$$\left(\frac{dC_{O2S} * V_S}{dt}\right)_{m.t.} = -\left(\frac{dC_{O2L} * V_L}{dt}\right)_{m.t.} \tag{46}$$

Replace dC_{O2S}/dt in equation (46) with the expression in equation (41) then isolate dC_{O2L}/dt to obtain the following equation.

$$\left(\frac{dC_{O2L}}{dt}\right)_{m.t.} = \frac{V_S}{V_L} * k_L a * \left(\frac{C_{O2S}}{H} - C_{O2L}\right) \tag{47}$$

The expression that describes the appearance of DHA in the liquid medium is the following.

$$\left(\frac{dC_{DL}}{dt}\right)_{rxn} = \frac{k*b*C_{O2L}}{K_m+C_{O2L}} \tag{48}$$

From stoichiometry, the rate of appearance of DHA is equal to twice the rate of disappearance of oxygen.

$$\left(\frac{dn_{O2L}}{dt}\right)_{rxn} = -\frac{1}{2}*\left(\frac{dn_{DL}}{dt}\right)_{rxn} \tag{49}$$

Convert equation (49) to concentration terms.

$$\left(\frac{dC_{O2L}*V_L}{dt}\right)_{rxn} = -\frac{1}{2}*\left(\frac{dC_{DL}*V_L}{dt}\right)_{rxn} \tag{50}$$

Replace dC_{DL}/dt in equation (50) with the expression in equation (48) then isolate dC_{O2L}/dt to obtain the following equation.

$$\left(\frac{dC_{O2L}}{dt}\right)_{rxn} = -\frac{1}{2}*\frac{k*b*C_{O2L}}{K_m+C_{O2L}} \tag{51}$$

Replace equations (47) and (51) into the mass balance expression in (44). Then the two simultaneous differential equations to be solved are the following.

$$\begin{aligned}\left(\frac{dC_{O2L}}{dt}\right)_{total} &= \frac{V_S}{V_L}*k_La*\left(\frac{C_{O2S}}{H}-C_{O2L}\right) - \frac{1}{2}*\frac{k*b*C_{O2L}}{K_m+C_{O2L}} \\ \left(\frac{dC_{O2S}}{dt}\right)_{total} &= -k_La*\left(\frac{C_{O2S}}{H}-C_{O2L}\right)\end{aligned} \tag{52}$$

The appearance of DHA in solution is described by equation (48). This differential equation is a linear combination of the two equations in (52) and is not required in order to solve the model. It has been included in the computer program for convenience because C_{DL} is the measured variable.

For the solution, the following numerical values were used and the results of the model, solved using MATLAB, are plotted below in figure 35 to 39. The MATLAB programs are included in the appendix.

k=	1.24e-3 mole DHA/g_{cell} min
b=	variable
K_m=	8.6e-6 mole O_2/L
$C_{O2L\phi}$=	0.3e-3 mole O_2/L
$C_{O2S\phi}$=	6.3e-3 mole O_2/L
$C_{DL\phi}$=	3.3e-3 mole DHA/L
H=	20
V_S=	from .015 to .035 L
V_L=	from .125 to .145 L
k_La=	variable

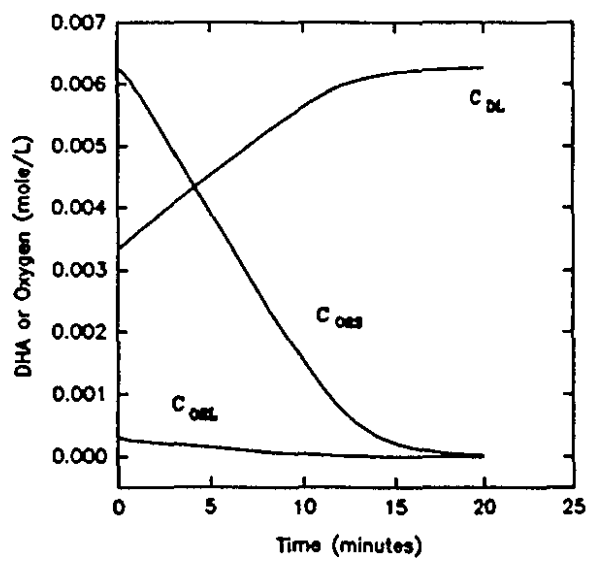

Figure 35. Model predictions for: C_{DL}, C_{O2S}, and C_{O2L} produced by *G. oxydans*. Oil volume is 25 ml of silicone microcapsules. Cell innoculum is 0.2 g cell/L. kLa is 10 1/min.

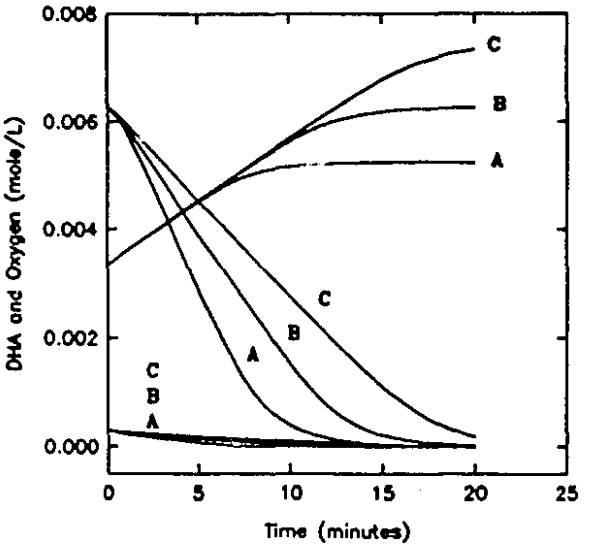

Figure 36. Model predictions for: C_{DL}, C_{O2S}, C_{O2L}, produced *G. oxydans*. Where oil volume is 15 (A), 25 (B), 35 (C) ml of microcapsules. cell innoculum is 0.2 g cell/L. kLa is 10 1/min.

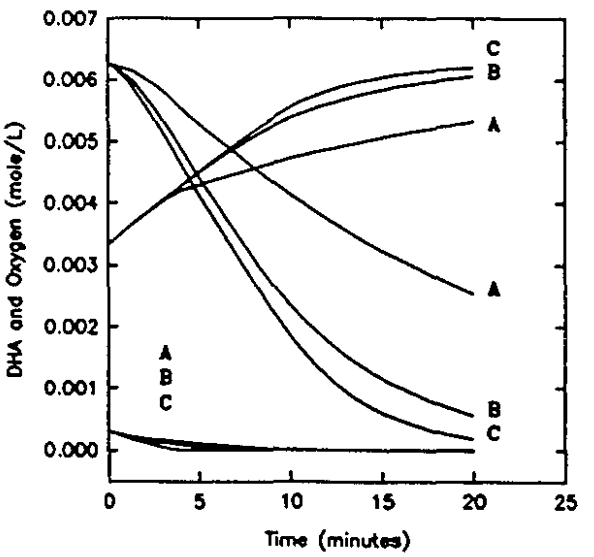

Figure 37. Model predictions for: C_{DL}, C_{O2S}, C_{O2L}, produced by *G. oxydans*. k_La is 1 (A), 3 (B), and 5 (C) min^{-1}. oil volume is 25 ml. cell innoculum is 0.2 g cell/L.

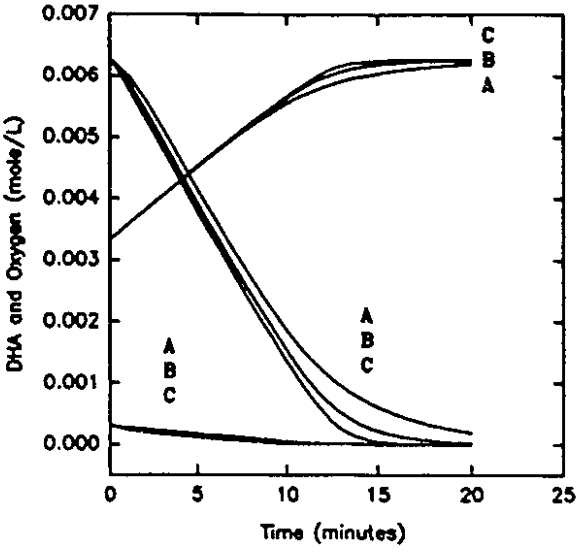

Figure 38. Model predictions for: C_{DL}, C_{O2S}, and C_{O2L} produced by *G. oxydans*. k_La is 5 (A), 10 (B), and 25 (C) min^{-1}. Oil volume is 25 ml. cell inoculum is 0.2 g cell/L.

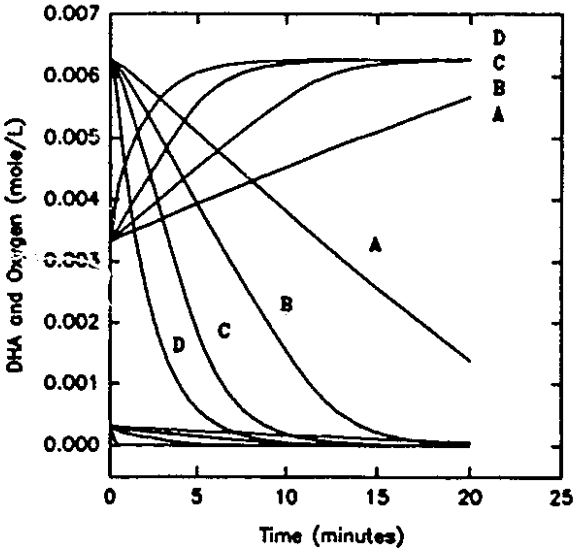

Figure 39. Model predictions for: C_{DL}, C_{O2S}, and C_{O2L}, produced by *G. oxydans*. cell inoculum is 0.1 (A), 0.2 (B), 0.4 (C), and 1.7 (D) g cell/L. oil volume is 25 ml. kLa is 10 1/min.

In figure 35 one can observe the path of a hypothetical fermentation. The cells produce DHA as they consume the oxygen in the liquid phase. Oxygen from the silicone oil microcapsules replenish the liquid medium. Once the total oxygen in the system has been consumed, the rate of DHA production falls to zero and the final equilibrium value is reached. As can be seen in figure 36, the final amount of DHA produced in a fermentation is dependant on the initial charge of microcapsules. The dependance of the rate of DHA production on the liquid film mass transfer coefficient can be observed in figures 37 and 38. As the value of k_La is increased, the rate of production of DHA also increases until it reaches a limit determined by the kinetics of the culture. In figures 37 and 38 the inoculum level is set at 0.2 g_{cell}/L, when k_La is higher than 3 min^{-1}, the solution approaches that which could be determined by using the simpler Kinetic Limitation model. At k_La values less than 3 min^{-1} the mass transfer begins to affect the overall observed rate. The relationship between the mass transfer coefficient and the inoculum level is also apparent in figure 39. As the amount of cells in the reactor is increased, the rate of DHA production increases, and similarly, the ability to remove the oxygen from the liquid phase is also increased. At high enough inoculum levels the mass transfer in the liquid film becomes the dominating rate as cells are figuratively waiting for the oxygen to transfer from the microcapsules to the liquid medium. At this point, the solution approaches that predicted by the simpler Liquid Film Mass Transfer Resistance model.

The relationship between the mass transfer resistance and the cell loading in the reactor can be seen in figure 40. The central area of the plot is the regime

where the full Combination Liquid Film Resistance and Kinetic Limitation model should be used, the relative rates of oxygen supply and demand in this area are of the same order. In the other two regimes, the combination model approaches the solutions predicted by either of the two simpler models because the relative rates of either oxygen supply or demand dominates the overall predicted rate.

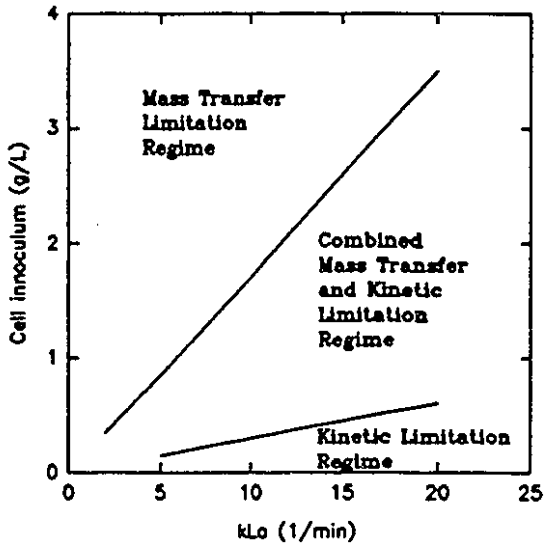

Figure 40. Regimes for the solutions of the Combined Liquid Film and Kinetic Limitation model.

4.2.4 Combination Internal and Liquid Film Mass Transfer Resistance Model

In the following model the internal diffusion of oxygen within the microcapsule is taken into consideration. The mass transfer of oxygen through the liquid film surrounding the microcapsule is included in the model as one of the boundary conditions. The cells are assumed to consume oxygen as fast as it is supplied to the liquid medium. Therefore the concentration of oxygen in the liquid

medium is assumed to be zero at all times. A schematic of the model can be seen in figure 41.

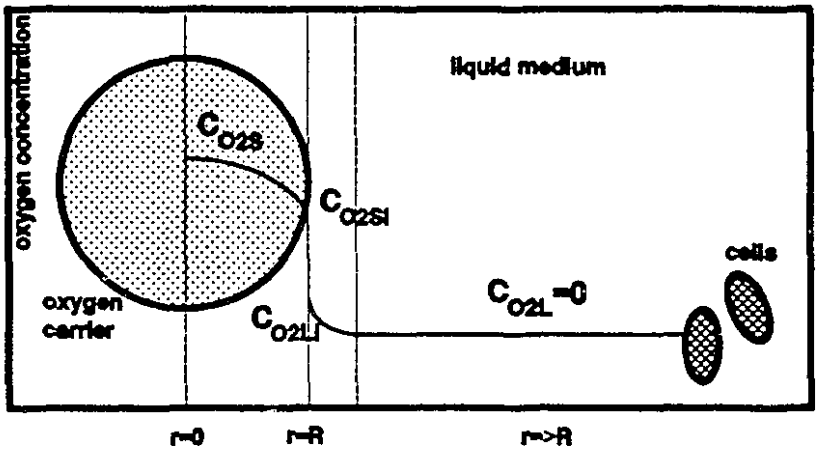

Figure 41. Schematic representation of Combination Internal and Liquid Film Mass Transfer Resistance model system.

The equation for diffusion in the radial direction in a sphere.

$$\frac{\partial C_{O2S}}{\partial t} = D_{O2S}\left(\frac{1}{r^2}\frac{\partial}{\partial r}\left(r^2\frac{\partial C_{O2S}}{\partial r}\right)\right) \tag{53}$$

Initial condition.

$$t = 0 \quad r = all\ r \quad C_{O2S} = C_{O2S\phi} \tag{54}$$

Boundary condition 1: no flux at midplane.

$$t = all\ t \quad r = 0 \quad \left(\frac{\partial C_{O2S}}{\partial r}\right)_{r=0} = 0 \tag{55}$$

Boundary condition 2: equate flux at interface.

$$t = all\ t \quad r = R \quad J_{O2S} = J_{O2L} \tag{56}$$

$$J_{O2S} = D_{O2S}*\frac{\partial C_{O2S}}{\partial r} = D_{O2L}*\frac{\partial C_{O2L}}{\partial r} = J_{O2L} \tag{57}$$

$$D_{O2S}\frac{\partial C_{O2S}}{\partial r} = \left(\frac{D_{O2L}}{\Delta r}\right)*(\Delta C_{O2L}) \tag{58}$$

$$D_{O2S}*\frac{\partial C_{O2S}}{\partial r} = k_L * (C_{O2Li}-C_{O2L}) \tag{59}$$

$$C_{O2Li}=\frac{C_{O2Si}}{H} \quad and \quad C_{O2L}=0 \tag{60}$$

therefore

$$t = all\ t \qquad r = R \qquad D_{O2S}*\left(\frac{\partial C_{O2S}}{\partial r}\right)_{r=R} = k_L a*\left(\frac{1}{a}\right)*\left(\frac{C_{O2Si}}{H}\right) \tag{61}$$

The partial differential equation above was solved numerically using a Galerkin weighted residual finite element method. The code was written in FORTRAN 77 and is included in the appendix. The following numerical values were used in the solution and the results are in figures 42 to 45.

$C_{DL\phi}$ = 3.3e-3 mole DHA/L
$C_{O2S\phi}$ = 6.3e-3 mole O_2 /L
$C_{O2L\phi}$ = 0.0 mole O_2 /L
D_{O2S} = 2.2e-9 m^2 /s
R = 50.0e-6 to 500.0e-6m
a = 3/R m^2/m^3
H = 20
V_S = 0.015 to 0.035 L
V_L = 0.125 to 0.145 L

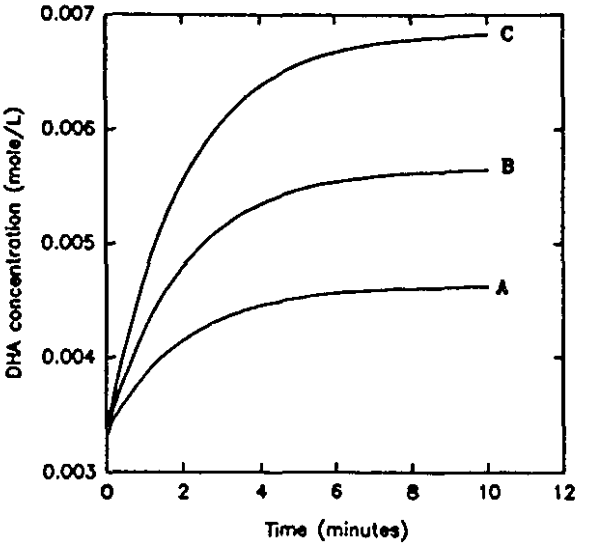

Figure 42. Model predictions of DHA produced by *G. oxydans* in non-growth medium with 15 (A), 25 (B) and 35 (C) mL microencapsulated silicone oil. kLa is 10 1/min.

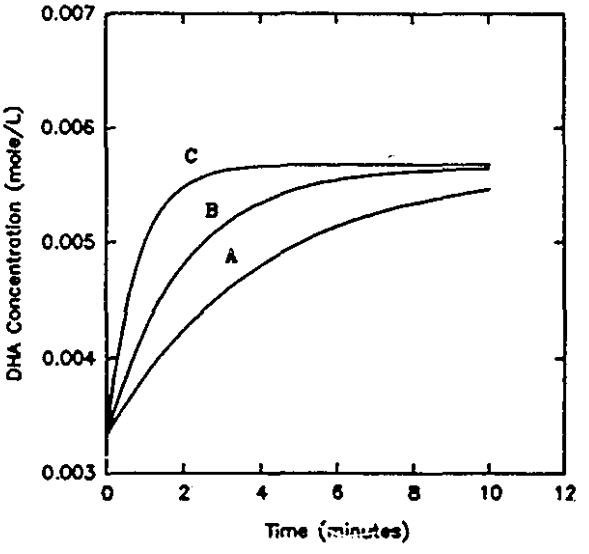

Figure 43. Model predictions of DHA produced by *G. oxydans* in non-growth medium where kLa is 5 (A), 10 (B), and 25 (C), min^{-1}. Microcapsule oil volume is 25 ml.

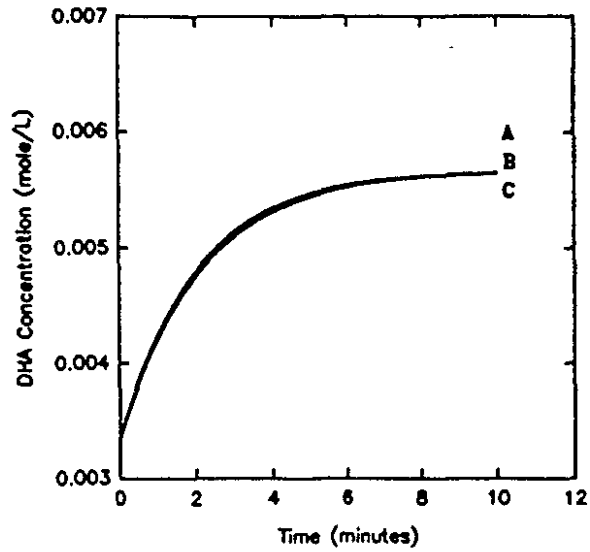

Figure 44. Model predictions of DHA produced by *G. oxydans* where microcapsule radius is 50 (A), 100 (B), and 500 (C) microns. Silicone oil volume is 25 mL, kLa is 10 1/min.

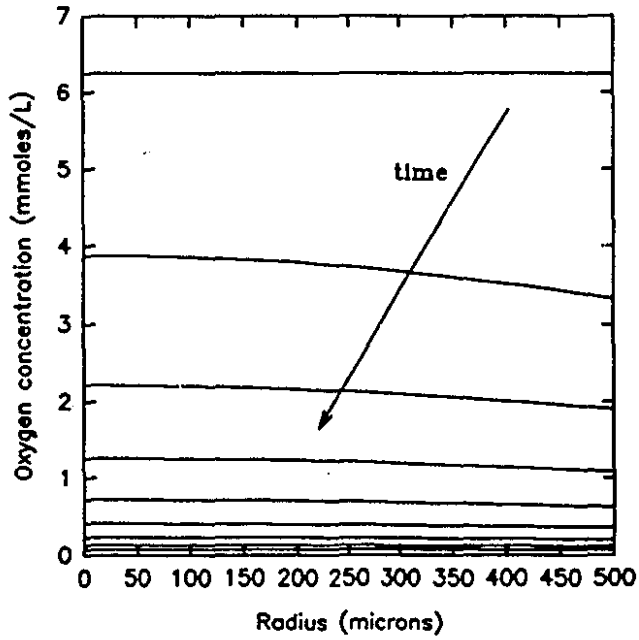

Figure 45. Model predictions for oxygen concentration variation within a single microcapsule at different times. Each curve is 1.2 min apart. Microcapsule radius is 500 microns. Total silicone oil volume is 25 mL, kLa is 25 1/min.

It is aparrent in figure 42 and 43 that the predictions of the Combined Internal and Liquid Film Mass Transfer Resistance model are identical to those obtained from the simpler Liquid Film Mass Transfer Resistance model on its own. The mass transfer within the microcapsule does not affect overall rate of DHA production which is dominated by the slower process occuring on the exterior of the microcapsule. There is no appreciable dependance of the appearance of DHA in the liquid medium on the radius of the bead as can be seen in figure 44. Figure 45 shows the concentration gradients of oxygen within the microcapsule as the fermentation progresses. The relatively flat oxygen concentration gradients within the microcapsule illustrates the fact that oxygen diffuses through the silicone oil quickly enough to maintain a constant concentration across the sphere.

5.0 DISCUSSION

G. oxydans has been used in the past as a benchmark to evaluate the oxygen transfer capabilities of a given reactor. The bioconversion of glycerol to DHA by the culture involves the incorporation of molecular oxygen without other supplemental requirements such as ATP, or NAD. Therefore the rate of production of DHA is assumed to be directly related to the consumption of oxygen. The ability to perform this bioconversion is maintained in medium that does not provide the components necessary for cell growth. In non-growth medium, the culture is effectively functioning as an immobilized enzyme. It was proposed in this work that the bioconversion of glycerol to DHA by resting *G. oxydans* could be used to evaluate the oxygen transfer from microencapsulated silicone oil.

In order for the bacteria to serve as a bioprobe for oxygen transfer, the culture would need to consume the dissolved oxygen in the liquid medium and immediately convert it to DHA. Any oxygen subsequently transfered from the oxygen carriers would be instantaneously scavenged by the cells in the production of DHA. This production of DHA would then be directly related to the rate of oxygen transfer.

The cells produce DHA at a rate governed by the kinetics of the enzyme responsible for the bioconversion. The currently accepted kinetics[40] of DHA production by resting *G. oxydans* is the following Michealis- Menten relationship that has been used throughout this work.

$$\frac{dC_{iL}}{dt} = \frac{k*b*C_{O2L}}{K_m+C_{O2L}} \qquad (62)$$

$$where \quad k\text{-}1.24e\text{-}3\frac{(moleDHA)}{(g_{cell}*\min)} \quad and \quad K_m\text{-}8.6e\text{-}6\frac{(moleO_2)}{L} \tag{63}$$

Since K_m is relatively small, unless the value of C_{O2L} is also small then the term

$$\frac{C_{O2L}}{K_m+C_{O2L}} \approx 1 \tag{64}$$

and therefore

$$\frac{dC_{DL}}{dt}\left(\frac{1}{b}\right) \approx k \tag{65}$$

Which means that the specific rate of DHA production is limited to the value of k.

The models developed for this system illustrate this theoretical limit of the cell culture. The solutions to the Combined Internal and Liquid Film Mass Transfer Resistance model are identical to the Liquid Film Mass Transfer Resistance only model. The mass transfer within the bead is faster than through the liquid film surrounding it and therefore it does not contribute significantly to the overall mass transfer resistance. This conclusion could also have been reached by calculating the Biot number for the system. The Biot number expressed in equation (66) is a dimensionless parameter relating the internal conductive to external convective mass transfer[16].

$$if \quad Bi\text{-}\frac{k_L*R}{D_{AB}} < 0.1 \quad ignore\ internal\ resistance \tag{66}$$

Multiply the top and bottom by the specific surface area "a".

$$a \approx \frac{A}{V} \approx \frac{3}{R} \tag{67}$$

$$Bi = \frac{k_L a * R^2}{3 * D_{AB}} < 0.1 \qquad (68)$$

$$k_L a < \frac{0.1 * 3 * D_{AB}}{R^2} = \frac{0.3 * (1.32e-7)}{(50e-6)^2} = 16 \text{ min}^{-1} \qquad (69)$$

For this system, it can be seen in equations 7 and 8 that internal mass transfer resistance can be neglected until $k_L a$ is larger than approximately 16 min^{-1}.

It is also apparent that at the inoculum levels used in this work, the solutions to the Combined Kinetic Limitation Mass Transfer Resistance model are identical to the simpler Kinetic Limitation model (fig. 36). At a $k_L a$ of approximately 3 min^{-1} and lower, the solutions produced by the two models diverge as mass transfer hinders the overall rate of DHA production. Therefore above $k_L a$ values of 3 min^{-1}, mass transfer through the film is faster than the kinetics of enzymatic reaction.

One can now arrange the three phenomena in order of importance to the net rate observed in the present study.

FASTEST				SLOWEST
Internal diffusion	>	Liquid Film	>	Cell Kinetics

From the models of the system, it appears that the cell kinetics will be the dominating process in the reactor.

Experiments in which the cell inoculum was varied (Table 2), show that the specific production rate remains constant at approximately 1e-3 (mole DHA/g_{cell}*L). This result corresponds to the value of k reported in the literature of 1.24e-3 [40]. Had the liquid phase oxygen concentration been reduced to zero by the cells and the rate

of oxygen transfer become limiting, and bacterial loading should not have affected the observed DHA production.

When reactor temperature was varied, the temperature dependence of the rate constant k in equation (62) may be seen. This dependence appears to follow the Arrhenius rule of thumb that for every 10°C increase, a doubling in reaction rate can be observed. Once again if mass transfer resistance were controlling, a variation with temperature should not have been observed[22]. This is another indication that it is the value of k and not k_La that determines the rate of DHA production.

The specific production rate of DHA shows no variation with the mixing speed under aerated reactor conditions (figures 21 and 22). Once again a rate of approximately 1e-3 mole DHA/g_{cell}*L is obtained. Since k_La is directly related to the level of mixing in a reactor [16], this observation again confirms that mass transfer resistance is not the limiting process. Therefore under normal bubble aeration conditions (1 vvm) and the inoculum levels used in this work, the oxygen supply is faster than the bacterial demand.

When oxygen is supplied from a microencapsulated silicone oil, the production of DHA has a profile similar to that observed using bubble aeration. As stated earlier, in order for the culture to provide an indication of mass transfer rates, liquid phase oxygen concentration should be reduced to zero within a very short time relative to the length of the experiment. Then for the remainder of the experiment, the mass transfer limited rate of oxygen supply would be reflected in the production of DHA. Otherwise, if oxygen is available in the liquid phase, then the DHA production rate will be determined by the rate constant k. Due to the fact that a

kinetic limitation is observed in the oxygen carrier experiments (fig. 25 and 26), this would imply that the cells consume the oxygen in the liquid phase, but oxygen from the microcapsules transfers to the liquid phase quickly enough to maintain a relatively high level of dissolved oxygen.

When experimental data from the non-growth production of DHA while varying the oxygen carrier loading (section 4.1.9) is overlaid on to the Kinetic Limitation model, one can see a reasonable correlation (fig. 46). All three experimental lines have similar slopes regardless of the oil volume in the reactor. This common slope is closely predicted by the Kinetic Limitation model. When the same data is compared to the Liquid Film Mass Transfer Resistance model (fig. 47), the data does not follow the model predictions of faster rates at higher oil volumes.

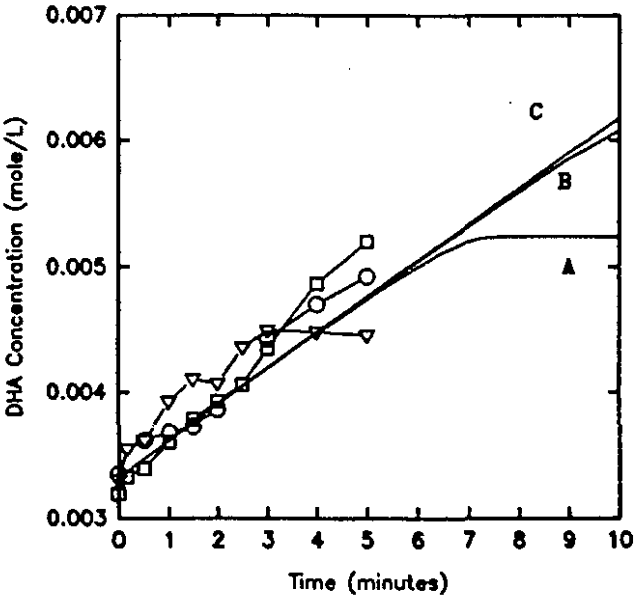

Figure 46. Experimental results from figure 26 overlaid on to model predictions of the Kinetic Limitation model. Inoculum level was 0.24 g cell/L. Oil volume is 15 (A,v), 25 (B,○), and 35 (C,□) ml.

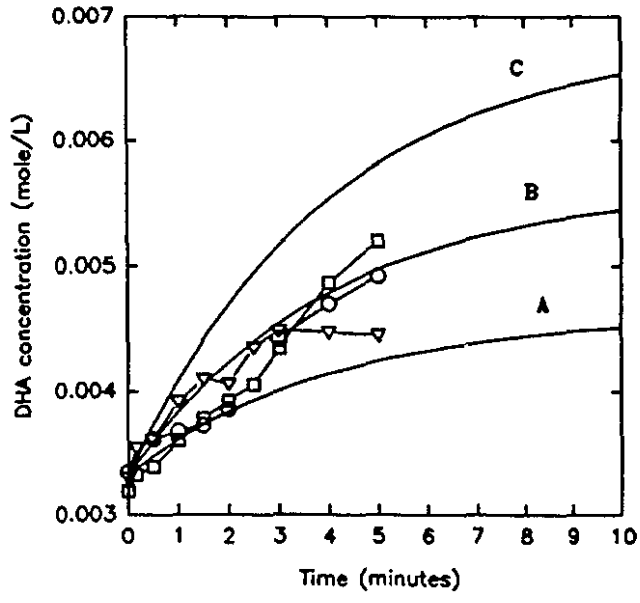

Figure 47. Experimental results from figure 26 overlaid on to model predictions by the Liquid film Mass Transfer Resistance model. kLa is predicted at 6 min^{-1}. Oil volume is 15 (A,▽), 25 (B,○), and 35 (C,□) ml.

Therefore the rate of DHA production is determined by enzyme kinetics rather than oxygen mass transfer from the oxygen carrier. It can be concluded that the kinetics of the cell culture governs the production of DHA, hence the system of resting *G. oxydans* used in this work did not serve as a suitable indicator of oxygen mass transfer rate. In fact the level of cell inoculum required in order for the system to acheive reasonable performance in the measurement of k_La is much higher than what is practical experimentally. The Combination Liquid Film Resistance and Kinetic Limitation model predicts the combinations of k_La and inoculum levels where

the system will be limited by mass transfer (fig. 40). The cell densities used in this work are much lower than those predicted to be necessary to perform the measurement of the mass transfer from the microcapsules. For instance, as can be seen in figure 40, if the k_La is expected to be 10 min^{-1}, then 1.7 g_{cell}/L of inoculum would be required to measure that k_La accurately. This amount of cells is 8 times that which was used in the present work.

In the non-growth fermentation experiments performed in this work a kinetic limitation was observed. According to the Combination Kinetic Limitation and Liquid Flim model, at the inoculum level used in this work (0.2 g_{cell}/L) any value of k_La greater than 3 min^{-1} would be limited by the kinetics of the cell culture. Therefore, the mass transfer coefficient of the liquid film surrounding the oxygen carriers must be greater than or equal to a minimum value of $k_La=3$ min^{-1}. Experiments performed in growth medium using *G. oxydans*[65] gave k_La values ranging between 2.3 and 4.3 min^{-1}. Hydrocarbon oil to water k_La values measured in three phase (oil, water, air) systems using *Candida rugosa*[24] and electrochemical techniques[51] reported values ranging from 1 to 10 min^{-1} respectively. Many other studies using silicone or perfluorocarbon oils reported higher cell growth rates or productivity when using oxygen carrier enhanced mediums; mass transfer rates were not reported[17,28,30,45,46,49,50,52,53]. Values of k_La encountered with conventional bubble aeration and mixing[2] range from 0.05 to 2 min^{-1}. Therefore, the mass transfer coefficients of microencapsulated silicone oil encountered in this work are in accordance with what has been previously reported, and this oxygen transfer performance ranges from equivalent to better than bubble aeration.

When comparing the non-growth production of DHA using microencapsulated silicone oil and solid silicone elastomer microspheres (fig. 24), the similar production rates of DHA obtained from the two oxygen carriers is an indication that the elastomer and oil possess similar oxygen transfer capabilities. It would therefore be preferable to use the larger and more robust solid spheres due to their physical strength and ease of separation from the liquid medium.

Further investigation into the k_La values of silicone oils and elastomers could be performed in reactors where the ratio of cell loading to the oxygen supplied is increased to operate in the mass transfer limitation regime. Continous operation of this reactor would allow production of DHA at levels that could be detected with minimal error using the analytical techniques available. Another approach would be to replace the cells with the glycerol dehydrogenase at levels necessary to measure k_La.

6.0 CONCLUSION

Dihydroxyacetone was produced in a non growth bio-conversion reaction from glycerol using *Gluconobacter oxydans*. The oxygen necessary for this reaction was supplied either with air or a silicone oxygen carrier. The conversion of glycerol to DHA was monitored in the reactor to determine the rate of oxygen supply to the culture from the oxygen carrier. Models of the reactor system were developed and compared to the experimental results. The results and theoretical predictions indicated that the rate of oxygen transfer to the liquid medium, was faster than the capabilities of the system to respond, indicating k_La values greater than a minimum of 3 min^{-1}. This minimum performance is equivalent to the best performance obtained from conventional sparging and mixing. The use of microencapsulated silicone oils and solid silicone elastomer microspheres could therefore be useful in the culturing of organisms that have a high demand for oxygen.

7.0 REFERENCES

1. Blakebrough, N. 1967. Biochemical and Biological Engineering Science, chapter 4: Agitation and aeration: by Finn, R.K. Academic Press. pp.69-99.

2. Atkinson, B., Mavituna, F. 1983. Biochemical Engineering and Biotechnology Handbook. MacMillan. Surrey, England. pp. 772.

3. Vant Riet, K. 1979. Review of measuring methods and results in nonviscous gas-liquid mass transfer in stirred vessels. Industrial Engineering Chemistry Process Design and Development. Vol. **18**. No. 3. pp. 357-364.

4. Treybal, R.E. 1980. Mass transfer operations. 3rd edition. McGraw Hill. pp. 23.

5. Krebs, W.M., Haddad, I.A. 1972. The oxygen electrode in fermentation systems. Developments in Industrial Microbiology. Developements in Industrial Micrbiology. vol. **13**. pp. 113-127

6. Linek, V., Vacek, V., Benes, P., Sinkule, J. 1989. Transient characteristics of oxygen probes with significant liquid film effects. Biotechnology and Bioengineering. vol. **33**. pp. 39-48.

7. Manfredini, R., Trilli, A. 1984. Measurement of the oxygen transfer capacity of fermenters: Theory and practice. Chimica e l'Industria (Milan). vol. 66. no. 5. pp.358-367

8. Holt, J.G., Krieg, N.R., Sneath, P.H., Staley, J.T., Williams, S.T. 1994. Bergey's Manual of Determinative Bacteriology. 9th edition. Williams and Wilkins. pp. 84.

10. Hauge, J.G., King, T.E., Chedelin, V.H. 1955. Oxidation of dihydroxyacetone via the pentose cycle in acetobacter suboxydans. Journal of Biological Chemistry. vol. **214**. pp. 11-26.

11. Bories, A., Claret, C., Soucaille, P. 1991. Kinetic study and optimization of the production of dihydroxyacetone from glycerol using *Gluconobacter oxydans*. Process Biochemistry. Vol. **26**. pp. 243-248.

12. Oosterhuis, N.M.G., Groesbeek, N.M., Kossen, N.W.F., Schenk, E.S. 1985. Influence of dissolved oxygen concentration on the oxygen kinetics of *Gluconobacter oxydans*. Applied Microbiolgy and Biotechnology. vol. **21**. pp. 42-49.

13. Tribe, L.A., Briens, C.L., Margaritis, A. 1995. Determination of the volumetric mass transfer coefficient (k_La) using the dynamic "gas-out-gas-in" method: Analysis of errors caused by dissolved oxygen probes. Biotechnology and Bioengineering. Vol. **46**. pp. 388-392.

14. Yamada, S., Nabe, K., Izuo, N., Wada, M., Chibata, I. 1979. Fermentative production of dihydroxyacetone in *Acetobacter suboxydans* ATCC 621. Journal of Fermentation Technology. vol. **57**. no. 3. pp. 215-220

15. King, T.E., Chedelin, V.H. 1952. Oxidative dissimilation in *Acetobacter suboxydans*. Journal of Biological Chemistry. Vol. **198**. pp. 127-133.

16. Geankoplis, C.J. 1983. Transport Processes and Unit Operations. 2nd edition. Allyn and Bacon. USA.

17. Mcmillan, J.D., Wang, D.I.C. 1990. Mechanisms of oxygen transfer enhancement during submerged cultivation in perfluorochemical-in-water dispersions. Annals of the New York Academy of Sciences. vol. **589**. pp. 283-300

18. Lewis, W.K., Witman, W.G. 1924. Principles of gas absorption. Industrial and Engineering Chemistry. vol. **16**. no. 12. pp. 1215-1220.

19. Bartholomew, W.H., Karow, E.O., Sfat, M.R., Wilhelm, R.H. 1950. Oxygen transfer and agitation in submerged fermentations: Mass transfer of oxygen in submerged fermentations of *Streptomyces griseus*. Industrial and Engineering Chemistry. vol. **42**. no. 9. pp. 1801-1809.

20. Aiba, S., Yamada, T. 1961. Oxygen absorption in bubble aeration, Part 1 and Part 2. Journal of General and Applied Microbiology. vol. **7**. no. 2. pp. 100-112.

21. Finn, R.K. 1954. Agitation-aeration in the laboratory and in industry. Bacterialogical Review. vol. **18**. pp.254-274.

22. Ramalho, R.S. 1983. Introduction to Wastewater Treatment Processes. 2nd edition. Academic Press. San Diego, California.

23. Blakebrough, N. 1967. Biochemical and Biological Engineering Science. Chapter 5: Mass transfer in fermentation equipment. by: Calderbank, P.H. Academic Press. pp. 101-180.

24. Yoshida, T., Yokoyama, K., Chen, K., Sunouchi, T., Taguchi, H. 1977. Oxygen transfer in hydrocarbon fermentation by *Candida rugosa*. Journal of Fermentation Technology. vol. **55**. no. 1. pp. 76-83.

25. Abu Reesh, I., Kargi, F. 1989 Biological responses of *Hybridoma* cells to defined hydrodynamic shear stress. Journal of Biotechnology. vol. **9**. pp. 167-178.

26. Augenstein, D.C., Sinskey, A.J., Wang, D.I.C. 1971. Effect of shear on the death of two strains of mammalian tissue cells. Biotechnology and Bioengineering. vol. **13**. pp. 409-418.

27. Oh, S.K.W., Nienow, A.W., Al-Rubeiai, M., Emery, A.N. 1989. The effect of agitation intensity with and without continuous sparging on the growth and antibody production of *Hybridoma* cells. Journal of Biotechnology. vol. **12**. pp. 45-62.

28. King, A.T., Mulligan, B.J., Lowe, H.C. 1989. Perfluorochemicals and cell culture. Bio/Technology. vol. **7**. pp. 1037-1042.

29. Bungay, H.R., Bungay, M.L., Haas, C.N. 1983. Annual Reports on Fermentation Processes. Chapter 6: Engineering at the micoorganism scale. Academic Press. pp. 149-174.

30. Damiano, D. Wang, S.S. 1985. Novel use of a perfluorocarbon for supplying oxygen to aerobic submerged cultures. Biotecnology Letters. vol. **7**. no. 2. pp. 81-86

31. Trinh, K., Garcia-Briones, M.A., Hink, F., Chalmers, J.J. 1994. Quantification of damage to suspended insect cells as a result of bubble rupture. Biotechnology and Bioengineering. vol. **43**. pp. 37-45.

32. Garcia-Briones, M.A., Chalmers, J.J. 1994. Flow parameters associated with hydrodynamic cell injury. Biotechnology and Bioengineering. vol. **44**. pp. 1089-1098.

34. Monahan, P.B., Holtzapple, M.T. 1993. Oxygen transfer in a bioreactor. Biotechnology and Bioengineering. vol. **42**. pp. 724-728.

35. Sucker, H.G., Jordan, M., Eppenberger, H.M., Widmer, F. 1994. Bubble bed reactor: A reactor design to minimize the damage of bubble aeration on animal cells. Biotechnology and Bioengineering. vol. **44**. pp. 1246-1254.

36. Holst, O., Enfors, S.O., Mattiasson, B. 1982. Oxygenation of immobilized cells using hydrogen-peroxide; a model study of *Gluconobacter oxydans* converting glycerol to dihydroxyacetone. European Journal of Applied Microbiology and Biotechnology. vol **14**. pp. 64-68.

37. Adlercreutz, P., Mattiasson, B. 1982. Oxygen supply to immobilized cells: 1. Oxygen production by immobilized *Chlorella pyrenoidosa*. Enzyme Microbiology Technology. vol. **4**. pp. 332-336.

38. Adlercreutz, P., Holst, O., Mattiasson, B. 1982. Oxygen supply to immobilized cells: 2. Studies on a coimmobilized algae-bacteria preparation with *in-situ* oxygen generation. Enzyme Microbiology Technology. vol. **4**. pp. 395-400.

39. Adlercreutz, P., Mattiasson, B. 1984. Oxygen supply to immobilized cells: 4. Use of p-benzoquinone as an oxygen substitute. Applied Microbiology Biotechnology. vol. **20**. pp. 296-302.

40. Adlercreutz, P. 1986. Oxygen supply to immobilized cells: 5. Theoretical calculations and experimental data for the oxidation of glycerol by immobilized *Gluconobacter oxydans* cells with oxygen or p-benzoquinone as electron acceptor. Biotechnology and Bioengineering. vol. **28**. pp. 223-232.

41. Barman, T.E. 1969. Enzyme Handbook. vol. 1. Springer. Berlin. Heidelberg.

43. Matthews, C.K., Holde, K.E. 1990. Biochemistry. Benjamin Cummings, California. pp. 216-243.

45. Adlercreutz, P., Mattiasson, B. 1982. Oxygen supply to immobilized cells: 3. Oxygen supply by heamoglobin or emulsions of perfluorochemicals. European Journal of Applied Microbiology Biotechnology. vol. **16**. pp. 165-170.

46. Chibata, I., Yamada, S., Wada, M., Izuo, N., Yamaguchi, T. 1974. Cultivation of aerobic microorganisms. U.S. Patent 3,850,753.

47. Rodnight, R. 1954. Manometric determination of the solubility of oxygen in liquid paraffin, olive oil and silicone fluids. Biochemistry Journal. vol. **57**. pp. 661-663.

48. Lee, J.H., Foster, N.R. 1990. Mass transfer and solubility of O_2 and CH_4 in silicone fluids. Industrial Engineering Chemistry Res. Vol. **29**. pp. 691-696.

49. Junker, B.H., Wang, D.I.C., Halton, T.A. 1990. Oxygen transfer enhancement in aqueous/perfluorocarbon fermentation systems: II. Theoretical analysis. Biotechnology and Bioengineering. vol. **35**. pp. 586-597.

50. Rols, J.L., Goma, G. 1989. Enhancement of oxygen transfer rates in fermentations using oxygen vectors. Biotechnology Advances. vol. **7**. pp. 1-14.

51. Rols, J.L., Condoret, J.S., Fonade, C., Goma, G. 1991. Modeling of oxygen transfer in water through emulsified organic liquids. Chemical Engineering Science. vol. **46**. no. 7. pp. 1869-1873.

52. Hamamoto, K., Tokashiki, M., Ichikawa, Y., Murakami, H. 1987. High cell density culture of a *Hybridoma* using perfluorocarbon to supply oxygen. Agricultural Biological Chemistry. vol. **51**. no. 12. pp. 3415-3416.

53. Van Sonsbeck, H.M., De Blanc, H., Tramper, J. 1992. Oxygen transfer in liquid-impelled loop reactors using perfluorocarbon liquids. Biotechnology and Bioengineering. vol. **40**. pp. 713-718.

54. Playne, M.J., Smith, B.R. 1983. Toxicity of organic extraction reagents to anaerobic bacteria. Biotechnology and Bioengineering. vol. **25**. pp. 1251-1265.

55. Poncelet, D., Leung, R., Centomo, L., Neufeld, R.J. 1993. Microencapsulation of silicone oils within polyamide-polyethylenimine membranes as oxygens carriers for bioreactor oxygenation. Journal of Chemical Technology Biotechnology. vol. **57**. pp. 253-263.

56. Miller, G.L., Blum, R., Glennon, W.E., Burton, A.L. 1960. Measurement of carboxymethylcellulase activity. Analytical Biochemistry. vol. **2**. pp. 127-132.

57. Chithambara Thanoo, B., Jayakrishnan, A. 1991. Tantalum loaded silicone microspheres as particulate emboli. Journal of Microencapsulation. vol. **8**. no. 1. pp. 95-101.

58. Fernandez, C.C. 1994. Oxidation of ferrous iron using silicone microspheres as oxygen carriers. Research Project and Seminar report, submitted to R.J. Neufeld, McGill University.

59. Adlercreutz, P., Holst, O., Mattiasson, B. 1985. Characterization of *Gluconobacter oxydans* immobilized in calcium alginate. Applied Microbiology Biotechnology. vol. **22**. pp. 1-7.

63. Hauge, J.G., King, T.E., Chedelin, N.H. 1955. Alternate conversions of glycerol in *Acetobacter suboxydans*. Journal of Biological Chemistry. vol. **214**. pp. 1-9.

65. Leung, R. 1992. Enhancement of oxygen transfer rate using microencapsulated silicone oils as oxygen carriers. M. Eng. Thesis. McGill University.

66. Battino, R. 1981. Solubility Data Series. vol. 7. Oxygen and Ozone. Pergammon Press. QD181.01 O95.

67. Chandler, D., Davey, M.R., Lowe, K.C., Mulligan, B.J. 1987. Effects of emulsified perfluorochemicals on growth and ultrastructure of microbial cells in culture. Biotechnology Letters. vol. 9. no. 3, pp. 195-200.

68. Buckels, R.G. 1966. An analysis of gas exchange in a membrane oxygenator. Phd thesis, Massachuesets Institute of Technology.

APPENDIX

Glossary of Abbreviations

a	specific area (m^2/m^3)
A	total area (m^3)
ATCC	American Type Culture Collection
ATP	adenosine triphosphate
b	cell loading (g cell/L)
b.k.	big Kahuna
Bi	Biot number
cs	centistoke
°C	degrees celcius
C	concentration -with subscripts (mole/L)
-subscripts	species: **O2** -oxygen, **D** -DHA
	phase: **S** -silicone, **L** -liquid, **T** -total
	other: **i** -interface, **ϕ** -time zero
d	derivative
d_{32}	deSauter mean diameter
D_{AB}	diffusivity of A in B (m^2/min)
D_{O2S}	diffusivity of O_2 in silicone oil (m^2/min)
DHA	dihydroxyacetone $CH_2OHCHOCH_2OH$
DHA3P	dihydroxyacetone-3-phosphate $CH_2OPCHOCH_2OH$
DNS	dinitrosalicylic acid
DO	dissolved oxygen
e	exponent $*10^x$
E	reaction extent i.e. number of moles reacted (moles)
FORTRAN	formula translation
g	grams
g	gravity 9.8 m/s^2
g_{cell}	grams of cells dryweight (g)
Gly	Glycerol $CH_2OHCHOHCH_2OH$
Gly3P	Glycerol-3-phosphate $CH_2OPCHOHCH_2OH$
h	hours
H	Henry's constant
J_A	molar flux of component A (mole/m^{2*}min)

k	rate constant (mole/ g cell*min)	
$k_L a$	liquid film volumetric mass transfer coefficient (min^{-1})	
K_m	Michealis constant (mole/L)	
k_x	mass transfer coeffiecient of film x (m/min)	
ln	natural logarithm	
L	liter	
M	molar (mole/L)	
ml	milliliter	
mm	millimeter	
mmole	millimole	
min	minutes	
min^{-1}	reciprocal minutes	
m.t.	mass transfer	
MW	molecular weight	
n	moles	-with subscipts (moles)
-subscripts	species:	**O2** -oxygen, **D** -DHA
	phase:	**S** -silicone, **L** -liquid, **T** -total
	other:	**i** -interface, **ϕ** -time zero
NAD	nicotinamide adenine dinucleotide	
nm	nanometer	
O_2	oxygen	
PVA	polyvinylalchohol	
r	radial position inside microcapsule (m)	
R	microcapsule radius (m)	
R^2	correlation coefficient	
rad	radian	
radar	radio detecting and ranging	
R1-R7	resistance to mass transfer	
rpm	revolutions per minute (2π rads/min)	
RTV	room temperature vulcanizable	
rxn	reaction	
t	time (min)	
tot	total	
vvm	volume per volume per minute	
v/v	volume per volume	
V	volume (L)	
x	distance (m)	

Kinetic Limitation Model

The following is the MATLAB M-file (saved on disk as kinetic.M) for the solution of the Kinetic Limitation Model:

```
function dc=ceco(t,cd)
k=1.243e-3;      b=0.4;              km=8.6e-6;
h=20;            col0=0.0003125;     cd0=3.33e-3;
vs=0.025;        vl=0.135;

dc=k.*b.*(2.*col0.*(h.*vs+vl)-vl.*(cd-cd0))./(2.*(h.*vs+vl))
   ./(km+(2.*col0.*(h.*vs+vl)-vl.*(cd-cd0))./(2.*(h.*vs+vl)));
```

The abbreviations in the M-file represent the following variables:

k	rate constant (moles DHA/g cell*min)
b	cell concentration (g cell/L)
km	Michealis constant (mole O_2/L)
h	Henry's constant
col0	initial liquid phase oxygen concentration (mole O_2/L)
cd0	initial liquid phase DHA concentration (mole DHA/L)
vs	silicone oil volume (L)
vl	liquid medium volume (L)
dc	accumulation of moles of DHA in the liquid phase (mole O_2/L*min)

The following text is the format of the input required at the MATLAB command line to run the simulation and save the output as a data file, followed by an example:

```
>[t,x]=ode45('filename', initial time, final time, C_DL4);
>save datafile.dat  t x -ascii

>[t,x]=ode45('kinetic', 0, 20, 0.00333);
>save sim_1.dat  t x -ascii
```

The data file has the following format:

time	DHA concentration
-	-
-	-
-	-
-	-

Combination Liquid Film Resistance and Kinetic Limitation Model

The following is the MATLAB M-file (saved on disk as lumpcap.M) for the solution of the Combination Liquid Film Resistance and Kinetic Limitation Model:

```
function ndot = lump(t,n)
ndot = zeros (3,1);

kla=10;
h  =.05;
k1 =6.22e-4;
k2 =1.243e-3;
b  =.4;
km =8.6e-6;
vs =.025;
vl =.135;


ndot(1) = ((vs./vl).*kla.*(h.*(n(2)./vs)-(n(1)./vl))
          -k1.*b.*(n(1)./vl)./(km+(n(1)./vl))).*vl;
ndot(2) = (-kla.*(h.*(n(2)./vs)-(n(1)./vl))).*vs;
ndot(3) = (k2.*b.*(n(1)./vl)./(km+(n(1)./vl))).*vl;
```

The abbreviations in the M-file represent the following variables:

kla	liquid film mass transfer coefficient (min^{-1})
h	Henry's constant
k1	0.5 * k2
k2	rate constant (moles DHA/g cell*min)
b	cell concentration (g cell/L)
km	Michealis constant (mole O_2/L)
vs	silicone oil volume (L)
vl	liquid medium volume (L)
ndot(1)	accumulation of moles of oxygen in the liquid phase (mole O_2/L*min)
ndot(2)	accumulation of moles of oxygen in the silicone phase (mole O_2/L*min)
ndot(3)	accumulation of moles of DHA in the liquid phase (mole O_2/L*min)
n(1)	moles of oxygen in the liquid phase (mole O_2/L)
n(2)	moles of oxygen in the silicone phase (mole O_2/L)

The following text is the format of the input required at the MATLAB command line to run the simulation. After which the output is converted to concentration terms, then output is arranged and lastly, saved as a data file. An example using the values that correspond to the numbers in the M file above follows.

```
>[t,x]=ode45('filename', initial time ,final time, [n_O2L, n_O2S, n_DL],tolerance);
>cl=x(:,1)/vl;  cs=x(:,2)/vs;  cd=x(:,3)/vl;
>turd=[t cl cs cd];
>save datafile.dat  turd  -ascii

>[t,x]=ode45('lumpcap', 0, 20, [0.0000421875, 0.00015625, 0.00044955], 1e-7);
>cl=x(:,1)/0.135;  cs=x(:,2)/0.025;  cd=x(:,3)/0.135;
>turd=[t cl cs cd];
>save sim_2.dat  turd  -ascii
```

The data file has the following format:

time	C_{O2L}	C_{O2S}	C_{DL}
-	-	-	-
-	-	-	-
-	-	-	-
-	-	-	-
-	-	-	-

Combination Internal and Liquid Film Mass Transfer Resistance Model

The following is the FORTRAN program that will solve the partial differential equation in the Combination Internal Resistance and Liquid Film Mass Transfer Resistance Model.

```
C
C THIS PROGRAM SOLVES THE DIFFUSION EQUATION IN SHERICAL COORDINATES USING
C THE GALERKIN WEIGHTED RESIDUAL FINITE ELEMENT METHOD
C
      IMPLICIT REAL*8 (A-H, O-Z)
      DIMENSION W(3), GP(3), X(11), CT(11), CTO(11), CTOO(11)
      DIMENSION CTP(11), SF(11), SK(11,11), DC(11), DI(11), PHI(2)
      DIMENSION PHIX(2)
C --- DEFINING THE MESH
      NE=10
      NP=NE+1
      DO 5 I=1,NP
5        X(I)=FLOAT(I-1)/FLOAT(NE)
C --- INPUT DATA FOR GAUSS QUADRATURE
      DATA W /0.27778D0,0.44444444444D0,0.277777778D0/
      DATA GP/0.1127016654D0,0.50D0,0.8872983346D0/
      T=0.0D0
      TT=0.0D0
      DTT=0.2D0
      CECO=0.01D0
C --- DEFINE INITIAL CONDITIONS
      DO 6 J=1,NP
         CT(J)=1.0D0
         CTO(J)=1.0D0
6        CTOO(J)=1.0D0
      CDL=3.33D0
C --- DEFINE PARAMETRIC DATA
      ERRORL=1.0D-6
      MAXK=30
      TMAX=20
      R=500D-06
      CO2S0=6.25D0
C --- C1 = DAB/(R)**2
      C1 =.528D0
C --- C2 = -KLA*P/(DAB*A*H)
      C2 =-0.31566D0
C --- C3 = 2*(VS/VL)*(KLA/H)
      C3 =0.18519D0
C --- PREDICTOR STEP WHEN CONVERGED SOLUTION HAS SATISFIED PROPERTIES
      DT=0.02D0
      DTO=0.02D0
      EPS=0.0001D0
148   DO 45 K=1,NP
         CTP(K)=CT(K)+DT*((CT(K)-CTO(K))/DTO)
         CTOO(K)=CTO(K)
         CTO(K)=CT(K)
45       CT(K)=CTP(K)
C --- ASSEMBLY
C --- INITIALIZE NEWTON-RAPHSON ITERATION COUNTER
60    JK=0
C --- INITIALIZE SK=0 AND SF=0
64    DO 35 N=1,NP
         SF(N)=0.0D0
         DO 35 N1=1,NP
35          SK(N,N1)=0.0D0
```

```
C --- LOOP OVER THE ELEMENTS
      JK=JK+1
      DO 100 I=1,NE
         DX=X(I+1)-X(I)
C --- LOOP OVER THE GAUSS POINTS
         DO 100 J=1,3
            CALL TFUNCT(GP(J),DX,PHI,PHIX)
            CON=0.0D0
            CONX=0.0D0
            TEMP=0.0D0
            TEMPX=0.0D0
            CONO=0.0D0
            TEMPO=0.0D0
            XGP=X(I)+GP(J)*DX
            DO 90 L=1,2
               L1=I+L-1
               CON=CON+PHI(L)*CT(L1)
               CONX=CONX+PHIX(L)*CT(L1)
90             CONO=CONO+PHI(L)*CTO(L1)
          DCON=(CON-CONO)/DT
C --- LOOP OVER THE BASIS FUNCTIONS
            DO 100 L=1,2
               L1=I+L-1
               SF(L1)=SF(L1)+DX*W(J)*((DCON-C1*(2.0D0/XGP*CONX))*PHI(L)
     R+C1*CONX*PHIX(L))
               DO 100 M=1,2
                  M1=I+M-1
                  SK(L1,M1)=SK(L1,M1)-W(J)*DX*((PHI(M)/DT-C1*(2.0D0/XGP*
     RPHIX(M)))*PHI(L)+C1*PHIX(M)*PHIX(L))
100   CONTINUE
C --- APPLY BOUNDARY CONDITIONS
      SF(NP)=SF(NP)-C1*C2*CT(NP)
      SK(NP,NP)=SK(NP,NP)+C1*C2
C --- CALL THE MATRIX EQUATION SOLVER ROUTINE
      CALL SOL(SK,SF,DC,NP)
      DO 110 I=1,NP
110      CT(I)=CT(I)+DC(I)
C --- CALCULATE THE EUCLIDEAN NORM OF DC
      ERROR=0.0D0
      DO 120 I=1,NP
120      ERROR=ERROR+DC(I)**2
      EUCLIN=DSQRT(ERROR)
C --- ERROR
      IF (EUCLIN.LT.ERRORL) GOTO 150
C --- ITERATION COUNTER
      IF (JK.GT.MAXK) GOTO 130
      GOTO 64
C --- MESSAGE OF NON CONVERGENCE
130   WRITE(*,140)
      WRITE(*,141) NE
140   FORMAT(1X,'PROGRAM DID NOT CONVERGE IN ',I3,'ITERATIONS')
141   FORMAT(1X,'USING A',I3,'ELEMENT MESH'/)
      STOP
150   IF (JK.GT.3) EPS=EPS*0.5D0
      IF (JK.EQ.3) EPS=EPS
      IF (JK.LT.3) EPS=1.2*EPS
C --- CALCULATE THE ERROR NORM
      DO 18 K=1,NP
18       DI(K)=(CT(K)-CTP(K))/2.0D0
         CMAX=0.0D0
         DNORM1=0.0D0
         DO 19 KA=1,NP
            IF (CT(KA).GT.CMAX) CMAX=CT(KA)
            DNORM1=DNORM1+DI(KA)**2
```

```
19     CONTINUE
       DNORM=DSQRT(((DNORM1/(CMAX**2)))/NP)
C --- CALCULATE NEW TIME STEP
       DTN=DT*DSQRT(EPS/DNORM)
       IF (DTN.GE.CECO) DTN=ceco
C --- TIME STEP CONTROL
       IF (DTN.GE.DT) GOTO 93
       ADT=0.8D0*DT
       IF (DTN.GE.ADT) GOTO 94
       DT=DT/2.0D0
       GOTO 149
93     DTOO=DTO
       DTO=DT
       DT=DTN
       GOTO 198
94     DTOO=DTO
       DTO=DT
       DT=DT
198    CONTINUE
C --- TIME
       T=T+DTO
       DCDLDT=C3*CTO(NP)*CO2S0
       CDL=CDL+DCDLDT*DTO
       IF (T.GE.TT) THEN
       TT=TT+DTT
       WRITE(*,199) T,CDL
199    FORMAT(/2F15.6/)
C --- PRINT DENORMALIZED VALUES
       DO 200 I=1,NP
          PX=X(I)*R
          PCT=CT(I)*CO2S0
          WRITE(*,300) PX,PCT
300       FORMAT(5F15.6)
200    CONTINUE
       ENDIF
C --- TIME CONTROL
       IF (T.GT.TMAX) STOP
       GOTO 148
C --- PRIDICTOR STEP WHEN CONVERGED SOLUTION IS RETURNED DUE TO A LARGE
C --- TIME
149    DO 113 K=1,NP
          CTP(K)=CTO(K)+DT*((CTO(K)-CTOO(K))/DTO)
113       CT(K)=CTP(K)
       GOTO 60
       END
C
C SUBROUTINE IMPLEMENTING LINEAR BASIS FUNCTION
C
       SUBROUTINE TFUNCT(GP,DX,PHI,PHIX)
       IMPLICIT REAL *8 (A-H, O-Z)
       DIMENSION PHI(2), PHIX(2)
       PHI(1)=1.0D0-GP
       PHI(2)=GP
       PHIX(1)=-1.0D0/DX
       PHIX(2)=1.0D0/DX
       RETURN
       END
C
C SUBROUTINE TO SOLVE AX=C TYPE PROBLEMS
C
       SUBROUTINE SOL(A,C,X,NEQ)
       IMPLICIT REAL*8 (A-H, O-Z)
       DIMENSION A(NEQ,NEQ), C(NEQ), X(NEQ)
C --- FORWARD REDUCTION PHASE
```

```
      DO 10 K=2,NEQ
      DO 10 I=K,NEQ
      R=A(I,K-1)/A(K-1,K-1)
      C(I)=C(I)-R*C(K-1)
      DO 10 J=K,NEQ
10    A(I,J)=A(I,J)-R*A(K-1,J)
C --- BACK SUBSTITUTION PHASE (RESULTS STORED IN X)
      X(NEQ)=C(NEQ)/A(NEQ,NEQ)
      DO 30 K=NEQ-1,1,-1
      X(K)=C(K)
      DO 20 J=K+1,NEQ
20    X(K)=X(K)-A(K,J)*X(J)
30    X(K)=X(K)/A(K,K)
      RETURN
      END
```

This program will compile on most FORTRAN compilers. The output has the following format:

time C_{DL}

position $C_{O2S}|_{r=R}$

\- -
\- -
\- -
\- -
\- -

time C_{DL}

position $C_{O2S}|_{r=R}$

\- -
\- -
\- -
\- -
\- -